ABSTRACT

Title of Document: **REACTIONS OF ZINTL ION (Pb_9^{4-}) WITH GOLD PRECURSOR ($Au(PPh_3)Cl$)**

Lingling Wang
Master of Science, 2006

Directed By: **Professor Bryan W. Eichhorn**
Department of Chemistry and Biochemistry

Transition metal main group clusters have been studied extensively as models for heterogeneous catalysts and metal surface reactions. Synthetic protocols are developed by using polyatomic main group clusters (Zintl ions) for making new bimetallic nano-catalysts. In this thesis, reactions of Group 14 Zintl ion cluster Pb_9^{4-} with the Au precursor $Au(PPh_3)Cl$ are studied. A new Pb-Au cluster $[Pb@Au_8]$ and Zintl ion Pb_5^{2-} have been isolated.

$[Pb@Au_8]$ are the first isolated highly symmetric Pb-Au cluster, which has remarkable unit cell dimensions (16.5 Å, 16.5 Å and 184.6 Å) compared with other Pb clusters. The Pb atom is placed in the equivalent distance from all Au atoms which forms a highly symmetric cube. XPS spectroscopy was used to demonstrate the existence of the Pb atom in the complex.

Zintl ion $[Pb_5]^{2-}$ has also been synthesized in this study. In previous literatures, no unambiguous resonances of Pb_5^{2-} anion in solution by ^{207}Pb NMR spectroscopy have been reported in the range from +2000 to -5500 ppm, the region where the ^{207}Pb resonances of lead clusters are normally expected to occur. Here, we present an exciting stable ^{207}Pb NMR signal for Pb_5^{2-}. Another signal is expected based on the

population

statistical calculation for two kinds of Pb atoms in Pb_5^{2-}. The ^{207}Pb NMR analysis also gives important knowledge about dynamic behavior of the cluster anions. At low temperature, the $[Pb_5]^{2-}$ anion showed no intramolecular exchange of the two kinds of Pb atoms.

REACTIONS OF ZINTL ION (Pb_9^{4-}) WITH GOLD PRECURSOR ($Au(PPh_3)Cl$)

By

Lingling Wang

Dissertation submitted to the Faculty of the Graduate School of the University of Maryland, College Park, in partial fulfillment Of the requirements for the degree of Master of Science 2006

Advisory Committee:
Professor Bryan W. Eichhorn, Chair
Associate Professor Amy S. Mullin
Assistant Professor Andrei Vedernikov

Table of Contents

Chapter 1

Introduction

1.1 Introduction

One major goal of the cluster science is to discover new clusters with special electronic and structural stabilities so that they can be used as seeds for larger clusters. Transition metal main group clusters have been studied extensively as models for heterogeneous catalysts and metal surface reactions.[1,2] It was proposed that reactions occurring on clusters might mimic those which take place on metal surfaces.[3] This could possibly lead to a deeper understanding of the behavior of metal surfaces in catalysis reactions of industrial importance such as the reforming of hydrocarbons or conversion of synthetic gas.

Nanoclusters are well-ordered and have a high ratio of atoms located on the surface,[4] which usually have high catalytic activity and selectivity. Some of the clusters are the metal cores of the series of larger cluster molecules, such as anticuboctahedron Rh_{13} core and icosahedron Au_{13} core, reported by Schmid and coworkers.[5] They also synthesized M_{55} core, the uncharged cluster molecule, $[Au_{55}(PPh_3)_{12}Cl_6]$, which is the first example of a well-defined ligand-stabilized nanocluster.[5] Moiseev et al.[6] reported the giant cationic cluster $Pd_{561}L_{60}(OAc)_{180}$, which was the first example of isolated nanocluster as an active catalyst in solution. Castelman et al.[7] presented experimental evidence for the charged magic number cluster $[Al_{13}]^{-1}$. Bowen et al.[8] presented KAl_{13}, an anionic icosahedral $[Al_{13}]^{-}$ core

with a K^+ located on the outer surface. Schnokel et al.[9] reported $[Al_{77}R_{20}]^{2-}$ (R = $N(SiMe_3)_2$), a highly symmetric metalloid aluminum cluster with negatively charged Al_{13} center. Schleyer et al.[10] identified $Al@Pb_{10}^{1+}$ and $Al@Pb_{12}^{1+}$ clusters in the gas phase by mass spectroscopy.

1.2 Zintl Ions

The main group polyanions, Zintl ions, can be used for the synthesis of transition metal binary complexes. As Zintl ions do not have H or C groups that are difficult to remove and there are large number of soluble Zintl ions isolated, they are ideal for the synthesis of these types of complexes. Further oxidation of these bimetallic complexes results in the formation of ligand free bimetallic alloys.[11,12]

Zintl ions, were discovered in the 1890's by Joannis,[13,14] Kraus[15,16] and Smyth[17] with the study of alkali metal plumbides. Kummer and Diehl[18] reported the first single crystal X-ray structure of polyatomic main group cluster $Na_4(en)_7Sn_9$. In 1976, Corbett and co-workers[19] reported the use of a macrocyclic ligand, 4,7,13,16,21,24-Hexaoxa-1,10-diazobicyclo[8,8,8] hexacosane (referred as 2,2,2,-crypt) as a sequestering agent for the alkali metal cations of the binary alloys. 2,2,2-crypt increases solubility of alkali metals by breaking the ion pairing of the alkali metal / Zintl ion alloys to enhance the crystallization of the Zintl ions. Various Group 14 and Group 15 Zintl salts and naked metal clusters were subsequently isolated such as E_9^{4-} (E = Sn[20,21], Ge[22,23], Pb[24]), Ge_9^{2-} [25] and E_7^{3-} (E = P[26,27], As[28], Sb[19,29]).

The pinictogen (group 15) Zintl ions tend to form polycyclic hydrocarbon-like structures such as nortricyclane E_7^{3-} (E = P, As, Sb). The hydrocarbon analogy resides in

the fact that E and E^- (E = P, As) are electronically equivalent to CH and CH_2, respectively.

In contrast to the electron precise group 15 polyatomic anions, the group 14 Zintl ions form electron deficient, boron-hydride-like structures, such as E_5^{2-}[30,31] (Figure 1.1a) and E_9^{3-}[32-34] (E = Ge, Sn, Pb) (Figure 1.1c)

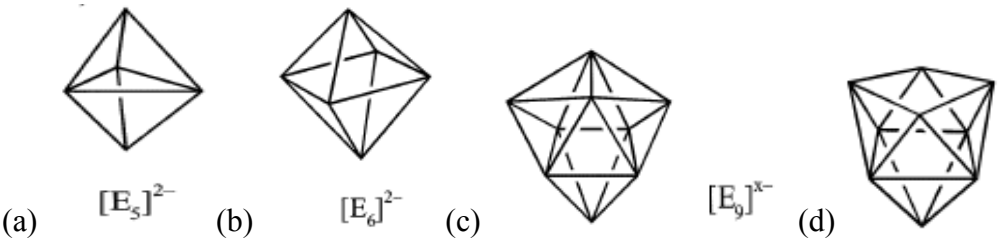

Figure 1.1. Structures of soluble homoatomic Group 14 anions a) $[E_5]^{2-}$, E = Ge, Sn, Pb; b) $[E_6]^{2-}$ in $[\{E\text{-}Cr(CO)_5\}_6]^{2-}$ with E = Ge, Sn; c,d) $[E_9]^{x-}$ (E = Si-Pb, x = 3,4) (taken from reference[35]).

Most commonly, the group 14 Zintl ions form deltahedral-like, nine atom clusters such as E_9^{4-} ion (E = Sn, Pb, Ge) in solution and in the solid state. These clusters usually crystallize in distorted, monocapped square antiprisms (C_{4v}) (Figure 1.1 d) and tricapped trigonal prisms (D_{3h}) (Figure 1.1 c).[35] The C_{4v}--C_{2v}--D_{3h} interconversion was proposed by Corbet et al.[35-37] The exchange mechanism involves bond formation across the open face of the cluster, followed by bond breaking. Similar to the borohydrides, in the case of electron deficiency, the elements could form either homoatomic multiple bonds or two-electrons-many-centers bonds. Due to the higher coordination number requirement, the later is more common for heavier members of Group 14 which form stable, naked,

ligand-free anions. Delocalized electrons are responsible for bonding within the deltahedral clusters; therefore, Wade-Mingos Rules are used for electron counting rather than the octet rule.[38] Wade's rules introduced the terminology of closo, nido, aracno and hypo type deltahedra to describe the structure of the cluster according to the number of vertex and overall charge of the cluster. For example, the E_9^{4-} has a nido structure, 2n+4 type (n = number of cluster verticies), with 9 vertices and 22 cluster electrons. On the other hand, the E_9^{2-} has 20 skeletal electrons, 9 vertices, thus the cluster is defined as a 2n+2 type and a closo geometry.

Ligand free Group 14 polyhedra have been studied extensively due to their simplicity and high reactivity. They react with transition metals to form transition metal / group 14 Zintl anions. One hundred years after the study of Joannis, Haushalter et al. structurally characterized the first transition metal-plumbide cluster, $[\eta^4 - E_9Cr(CO)_3]^{4-}$ anions[39] (E = Pb, Sn), which have capping $Cr(CO)_3$ unit on the open face of the E_9 cluster resulting closo geometry. Eichhorn et al. have reported the solution dynamics of the closo-$[Sn_9M(CO)_3]^{4-}$ where M = Cr, Mo, W as well as their synthesis, structures and properties[40]. They described the new isomeric form of the anions and showed equilibrium between η^4 and η^5 isomers by the way of ^{13}C and ^{119}Sn NMR spectroscopy.

Further studies have showed that nine-atom cluster can accommodate a central transition metal. Eichhorn et al. have prepared $[Sn_9Pt_2(PPh_3)]^{2-}$[41] and $[Sn_9Ni_2(CO)]^{3-}$ Zintl anions. They contain ligated transition metal fragments, $Pt(PPh_3)$ and Ni(CO), incorported into the transition metal centered anion frameworks as a vertex of the cluster. Although the Pt centered anion has a highly distorted Sn_9 cluster, the Ni centered one possesses an undistorted, C_{4v} closo structure. Besides the synthesis, structures and

characterization, the solution dynamics of $[Sn_9Pt_2(PPh_3)]^{2-}$anion were studied by ^{31}P and ^{119}Sn NMR spectroscopy. It has been shown that Sn_9 cluster is highly fluxional, on the other hand Pt-Pt-PPh_3 unit remains intact and it is not in exchange on the NMR time scale. $[Sn_9Ni_2(CO)]^{3-}$is a rare example of a paramagnetic Zintl ion complex. Due to its paramagnetic nature, the dynamic behavior of this complex could not be reported.

New group 14 Zintl ions, having frameworks other than E_9 cluster, are also stabilized by the transition metal. Huttner et al. reported octahedral E_6^{2-} unit in closo – $[E_6\{M(CO)_5\}_6]^{2-}$ (E = Sn, Ge) and (M = Cr, Mo, W).[42,43] These complexes were prepared from the reduction of EX_2 (GeI_2, $SnCl_2$) with $M_2(CO)_{10}^{2-}$ (M = Cr, Mo, W) in THF solutions. Studies by Eichhorn et al. showed a cyclohexane-like Sn_6^{12-} Zintl ion exist in closo-$[Sn_6\{Nb(tol)\}_2]^{2-}$ anion. Six-membered ring of tin atoms Nb(tol) fragments, forming distorted cube with two Nb atoms at opposite corners.[11]

The metal stabilized group 14 Zintl ions have become an active research area due to their potential application in the preparation of catalytically active binary alloys and nanomaterials.[37,44] It has been a goal to prepare ligand free transition metal / main group binary anions to enhance the catalytic activity. Recent studies have shown that employing metal precursors with more labile ligands is the most efficient way to prepare ligand-free transition metal / Zintl ion clusters. Although extensive theoretical studies have been reported on the metallated Zintl ions, very little structural data has been reported. In 2004, Eichhorn and co-workers[45] reported the free-standing naked icosahedral cluster, $[Pt@Pb_{12}]^{2-}$, that contains a Pt atom centered in a closo-$[Pb_{12}]^{2-}$ icosahedral Zintl ion with virtual I_h point symmetry. Recently Sevov et al.[46] succeeded in preparing a ligand-free, eighteen atom single-cage deltahedron of germanium atoms, centered by dimmer of

palladium atoms. $[Pd_2@Ge_{18}]^{4-}$ is made of two nine-atom germanium clusters, forming an oblong shape 18-vertex deltahedron. Subsequently, a cluster of eighteen Ge atoms enclosing trimer of Ni atoms have been prepared[47]. The ligand-free anion, $[Ni_3Ge_{18}]^{4-}$, contains two Ni centered Ge_9 clusters connected by a central Ni atom which plays a role as both inversion center and vertex for each cluster.

1.3. Gold clusters

Gold clusters and nanoparticles have become an active research field lately because of the discovery of remarkable catalytic properties of nanogold[48] and their potential applications in nanoelectronics, nanosensors, and as biological markers.[49] The chemistry of gold is dominated by the strong relativistic effects[50] and the so-called aurophilic attraction,[51] leading to highly unusual structures for gold clusters and compounds relative to those for copper and silver. Some exciting discoveries in elemental gold clusters have been reported, such as the tetrahedral Au_{20} cluster[52,53] , the golden fullerene Au_{32} cage cluster.[54,55]

Despite the fact that the bare 13-atom gold cluster anion has been shown not to possess a high symmetry icosahedral (I_h) structure,[56] Pyykko and Runeberg[57] recently presented a series of highly stable gold clusters containing an icosahedral Au_{12} cage and a central heteroatom, $M@Au_{12}$ (M = Ta-, W, Re+). They are valent isoelectronic to the known Ih Au_{13}^{5+} cage.[58,59] Mo, V and Nb analogs of this cluster have also been reported by the same group.[60.61]

Ligand-stabilized metal clusters are considered to be model compounds for the catalytic properties of very small metal particles as well as potential basic devices for the ultimate miniaturization in electronics. A preparation of small phosphine-stabilized gold

clusters was described by Schmid et al. in 1981.[62] It involves the reduction of $Au(PPh_3)Cl$ with diborane to yield a gold cluster typically formulated as $Au_{55}(PPh_3)_{12}Cl_6$, where the 55 gold atoms form a two-shell cuboctahedron with a ccp arrangement. Each of the 12 corner atoms would be bound to a phosphine ligand, while the six chloride ligands would be located at the central gold atom of the six square planes.

During the 1960's, Pt on alumina (Al_2O_3) was the most commonly used reforming catalyst.[84] The $PtM^{[1]}$ alloys, where M is a main group or transition metal (i.e. PtSn, PtAu systems), can be used for CO oxidation in Fuel cells,[85,86] such as Pt-Ge catalysts.[2,3,87] Addition of Pb to Al_2O_3 supported Ni or Pd was also reported.[88,89] These studies indicate that the transition metal/group 14 alloyed bimetallic catalysts have desirable properties for many catalytic processes.

$PtAu_x$ clusters have shown a variety of novel structures and interesting reactivity[63-73]. Mixed-metal clusters of this type are of potential importance in many areas. For example, such clusters may serve as models for bimetallic surface catalysts or as supported catalyst precursors themselves[74-77].

Shulga and co-workers[78] reported the XPS studies on ligand stabilized mixed-metal platinum-gold cluster compounds. Mason and co-workers[79,80] measured and interpreted the acetonitrile solution electronic absorption and magnetic circular dichroism (MCD) spectra for a variety of centered gold cluster complexes, including $M(AuPPh_3)_8^{2+}$, M = Pd or Pt (D_{4d} centered crown structure, figure 1.2-1) and $Au(AuPPh_3)_8^{3+}$ (D_{2h} centered icosahedral fragment structure, figure 1.2-2).

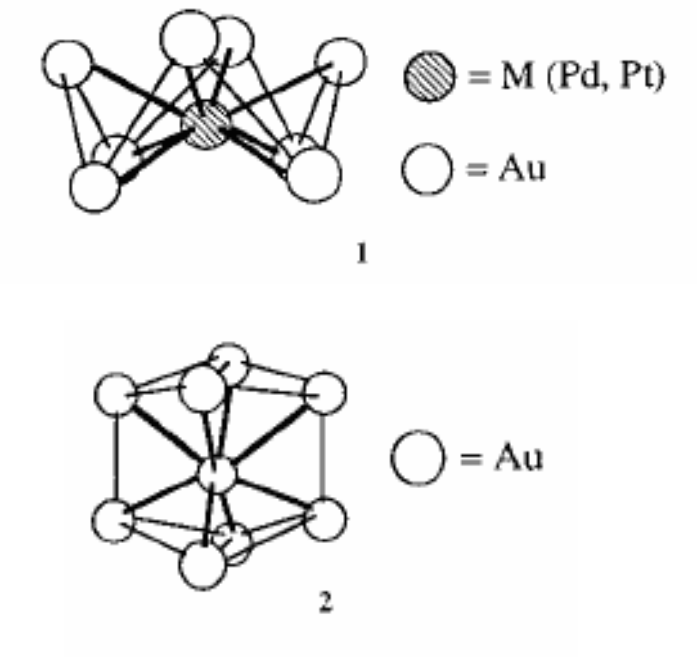

Figure 1.2. Centered gold cluster complexes 1) $M(AuPPh_3)_8^{2+}$, M = Pd or Pt; 2) $Au(AuPPh_3)_8^{3+}$ (Taken from reference[81])

Vollenbroek and co-workers also did a lot of work on gold clusters. They found that chemical analyses and conventional spectroscopic methods (e.g., IR) were of limited use to identify and to verify purity of gold clusters. ^{31}P NMR spectroscopy, however, proved to be very useful and became the main analytical tool in their work. This technique was also used to investigate reactions of gold-phosphine clusters[82,83] and to obtain information about chemical bonding and dynamical properties of these compounds.

1.4. Overview of the Thesis

In the following chapters of this thesis, the reactions of Group 14 Zintl ion cluster Pb_9^{4-} with the Au precursor PPh_3AuCl are studied.

Chapter 2 presents the synthesis, structure and characterization of the first high symmetric Pb-Au cluster [Pb@Au_8]. Chapter 3 gives the synthesis, structure and exciting NMR studies on cluster Pb_5^{2-}.

Chapter 2

[Pb@Au_8]

2.1. Introduction

In 1980 Vollenbroek and co-workers presented[90] the $^{31}P[^{1}H]$ NMR spectra of gold-phosphine clusters—$Au_8(PAr_3)_8^{2+}$, $Au_9(PAr_3)_8^{3+}$, $Au_{11}(PAr_3)_7X_3$, and $Au_{11}(PAr_3)_8Y_2^{+}$ (X = SCN, I; Y = SCN, Cl).(table 2.1) $Au_9(PAr_3)_8^{3+}$ was prepared by the reduction of $Au(PAr_3)NO_3$ with $NaBH_4$.[91] And $Au_8(PAr_3)_8^{2+}$ was prepared by the reaction of $Au_9(PAr_3)_8^{3+}$ with an excess of PAr_3.[83](Figure 2.1)

The proton-decoupled ^{31}P NMR spectra ($^{31}P[^{1}H]$ NMR) of all investigated gold-phosphine clusters show only one singlet, which is explained by a dominant trans influence of the central gold atom upon the chemical shifts of phosphines coordinated to peripheral gold atoms. All singlets are very sharp (line width 3 Hz) except for the singlet of $[Au_8L_8]^{2+}$ (L = PPh_3), which is rather broad (line width 25Hz) at room temperature, and does not show further broadening or sharpening on cooling (CD_2Cl_2).

Table 2.1. $^{31}P[^{1}H]$ NMR Data of Gold-Phosphine Clusters, Mononuclear Gold Complexes, and Free Phosphines (taken from reference [84])

	NMR, ppm[a]	
compd	C_6D_6	CD_2Cl_2
$Au_{11}[PPh_3]_7(SCN)_3$	+49.5	49.9
$Au_{11}[P(p\text{-}ClC_6H_4]_7(SCN)_3$	+48.0	
$Au_{11}[P(p\text{-}MeC_6H_4)_3]_7(SCN)_3$	+48.0	
$Au_{11}[P(p\text{-}ClC_6H_4)_3]_7I_3$	+48.2	
$Au_{11}[P(p\text{-}FC_6H_4)_3]_7I_3$	+47.5	
$[Au_{11}(PPh_3)_5(SCN)_2]PF_6$		+50.7
$[Au_{11}(PPh_3)_5Cl_2]PF_6$		+50.2
$[Au_9(PPh_3)_5](PF_6)_3$		+54.8
$[Au_9(P(p\text{-}MeC_6H_4)_3)_5](PF_6)_3$		+53.5
$[Au_8(PPh_3)_8](PF_6)_2$		+53.0
$Au(PPh_3)NO_3$		+25.1
$Au(PPh_3)Cl$		+31.0
$Au(PPh_3)SCN$		+34.8
$[Au(PPh_3)_2]PF_6$		+42.6
PPh_3	-8.3	
$P(p\text{-}ClC_6H_4)_3$	-11.4	
$P(p\text{-}MeC_6H_4)_3$	-10.8	
$P(p\text{-}FC_6H_4)_3$	-11.8	

[a] Relative to $OP(OMe)_3$ (TMP) reference (upfield = minus); all singlets apart from the septet of PF_6.

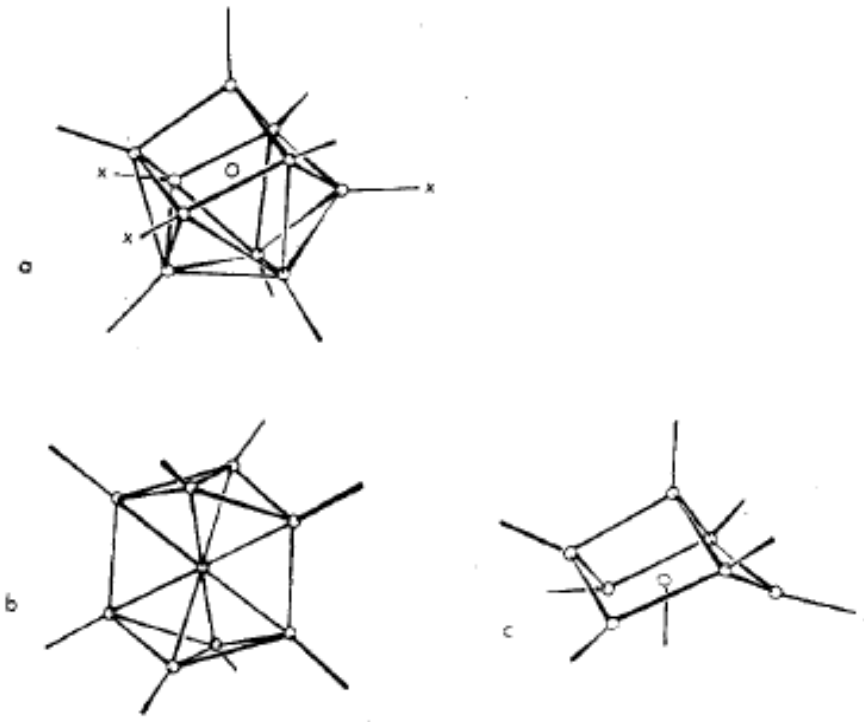

Figure 2.1. (a) $Au_{11}L_7X_3$; for $Au_{11}L_8Y^{2+}$ one of the X ligands is substituted by a L. (b) $Au_9L_8^{3+}$. (c) $Au_8L_8^{2+}$ (taken from reference [90])

Meanwhile, Vollenbroek's group[92] also presented results of XPS measurements of several Au_9, Au_{11} clusters and a new cluster compound containing eight gold atoms. They have stated that there is a close similarity between the XPS of gold(I) phosphine compounds and that of the gold cluster complexes. This result supports the description of the peripheral gold atoms as being linearly hybridized.

In 1982 Shulga and co-workers[93,94] reported the XPS studies on some gold clusters such as $[Au_9(PPh_3)_8](NO_3)_2$ (1.8 eV) and $[Au_{11}(PPh_3)_7I_3]$ (1.9 eV). These gold clusters are gold centered and expected to give different Binding Energy (E_b) for the central and peripheral gold atoms. In 1992, they further[78] presented the XPS studies on ligand stabilized mixed-metal platinum-gold cluster compounds. They reported that the Au $4f_{7/2}$

E_b's in all cluster compounds (range 84.57-85.07 eV) are shifted to higher values compared to that of metallic gold (84.20 eV for Au(0)), but are lower than in $AuPPh_3NO_3$ and $AuPPh_3Cl$ (85.37 and 85.55 eV for Au(1)). They are in the same range found for gold cluster compounds examined previously[93-95]. The Au $4f_{7/2}$ E_b's for all of the cluster compounds are close. This indicates that the Au atoms have similar electron densities, and the effective charge of Au in the cluster compounds is between those of Au(0) and Au(I). The E_b of Au $4f_{7/2}$ is determined primarily by the gold-phosphine and gold-gold interactions.

Mason and co-workers[79,80] measured and interpreted the acetonitrile solution electronic absorption spectra for a variety of centered gold cluster complexes, including $M(AuPPh_3)_8^{2+}$, M = Pd or Pt and $Au(AuPPh_3)_8^{3+}$.

The similarity of the energies of the Pt 5d orbitals suggests very weak "ligand field" effects from the surrounding peripheral Au atoms. It is consistent with the view that these orbitals are essentially nonbonding and localized on the Pt atom in the center of the cluster complex. Consequently the Pt 5d orbitals would be exposed along the 4-fold axis of the D_{4d} structure where they would provide electron density in that direction. This feature may help explain why the $Pt(AuPPh_3)_8^{2+}$complex is more reactive[96] when addition of electrophilic reagents (CO, H_2, D_2, CN-R, Hg(0), -HgCl, etc.) than $Au(AuPPh_3)_8^{3+}$. Such electrophiles would be attracted to the accessible 5d electron density of the Pt(0) center in the cluster complex.(Figure 2.2)

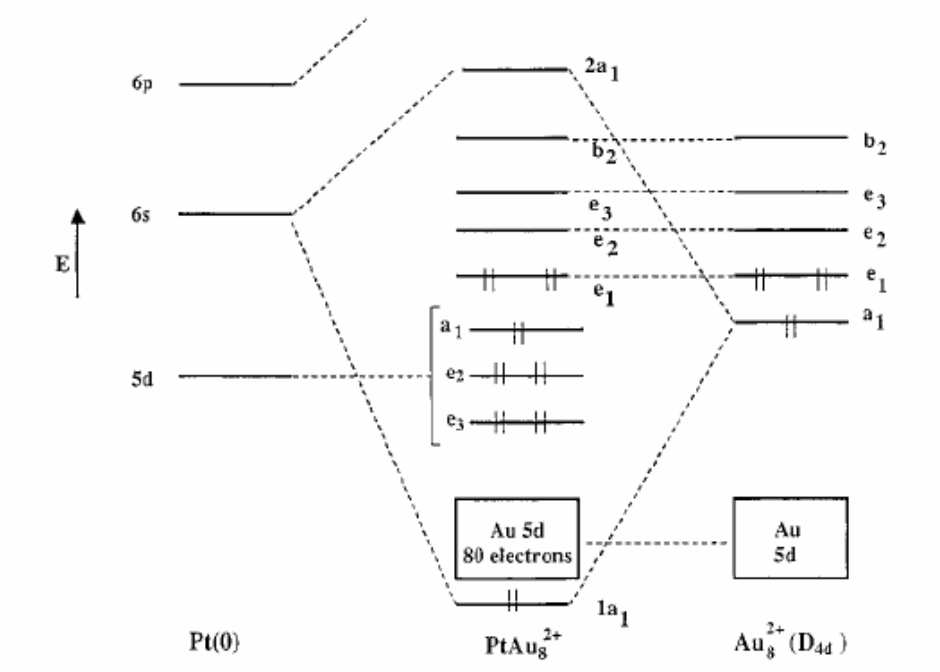

Figure 2.2. Simplified molecular orbital energy level scheme for $Pt(AuPPh_3)_8^{2+}$ assuming D_{4d} symmetry for the $PtAu_8^{2+}$ framework. (taken from reference [81])

To our knowledge, no Pb-Au Clusters have been reported. In this chapter, the reaction of Pb_9^{4-} Zintl ion with Au(I) precursor $Au(PPh_3)Cl$ is presented. The synthesis, structure and characterization of $PbAu_8$ are discussed. This high symmetric Pb-Au cluster comprises a Pb centered Au_8 cubic ion and posseses virtual O_h point symmetry.

2.2. Results and Discussion

2.2.1. Synthesis

Ethylenediamine (en) solutions of K_4Pb_9 react with KBH_4 and en solutions of PPh_3AuCl in the presence of 4 equivalence of 2,2,2-crypt to give [Pb@Au_8] clusters in a salt of proposed formula. The [Pb@Au_8] crystals are red-brown plates in appearance and

stable at least in mineral oil. While the $Pb@Au_8(PPh_3)_8$ portion of the X-ray structure is very well defined, the identity of the counter ion remains unknown.

The cluster has been characterized by single crystal XRD, energy dispersive X-Ray (EDX) analysis, ^{207}Pb NMR, ^{31}P NMR, XPS and ESI-MS.

2.2.2. Solid State Structure

Each of the crystal unit cells contains a non-interacting $[Pb@Au_8]$ cluster with one PPh_3Cl^+ cation. There are en solvent molecules in the crystal lattice. The salt is trigonal space group R-3c, and is shown in Figures 2.3 & 2.4.

Summaries of the crystallographic data and selected bond distances and angles for the cluster are given in Table 2.2, Table 2.3, Table 2.4, respectively.

The $[Pb@Au_8]$ complex has remarkable unit cell dimensions (16.5 Å, 16.5 Å and 184.6 Å) compared with other Pb clusters (table 2.5). Eight surface Au atoms form a cubic cage encapsulating the Pb atom at the center. The clusters possess virtual molecular O_h point symmetry. The Pb atom is placed in the equivalent distance from all Au atoms which forms a highly symmetric cube. The Au-Au contacts (2.99 Å, avg) are in agreement with the ones reported from MAu_8 (M = Pt, Pd)[80], and Au_9,[81] where the distances vary between 2.93 Å and 3.08 Å. The Au-P bond distances within the cluster average 2.28 Å and are similar to other Au complexes.[81,90,91] In comparison with $PtAu_8$[80] (D_{4d} centered crown structure), the angles of $(Au\text{-}Au\text{-}Au)_{avg}$ and P(1)-Au(1)-Pb in complex $[Pb@Au_8(PPh_3)_8]$ are 89.7° and 180° respectively, which confirmed the cubic structure given by Single Crystal X-ray (XRD) data. To our knowledge, there is no similar Pb compound reported in the literature which could be used for comparison of the Pb-Au bond distances.

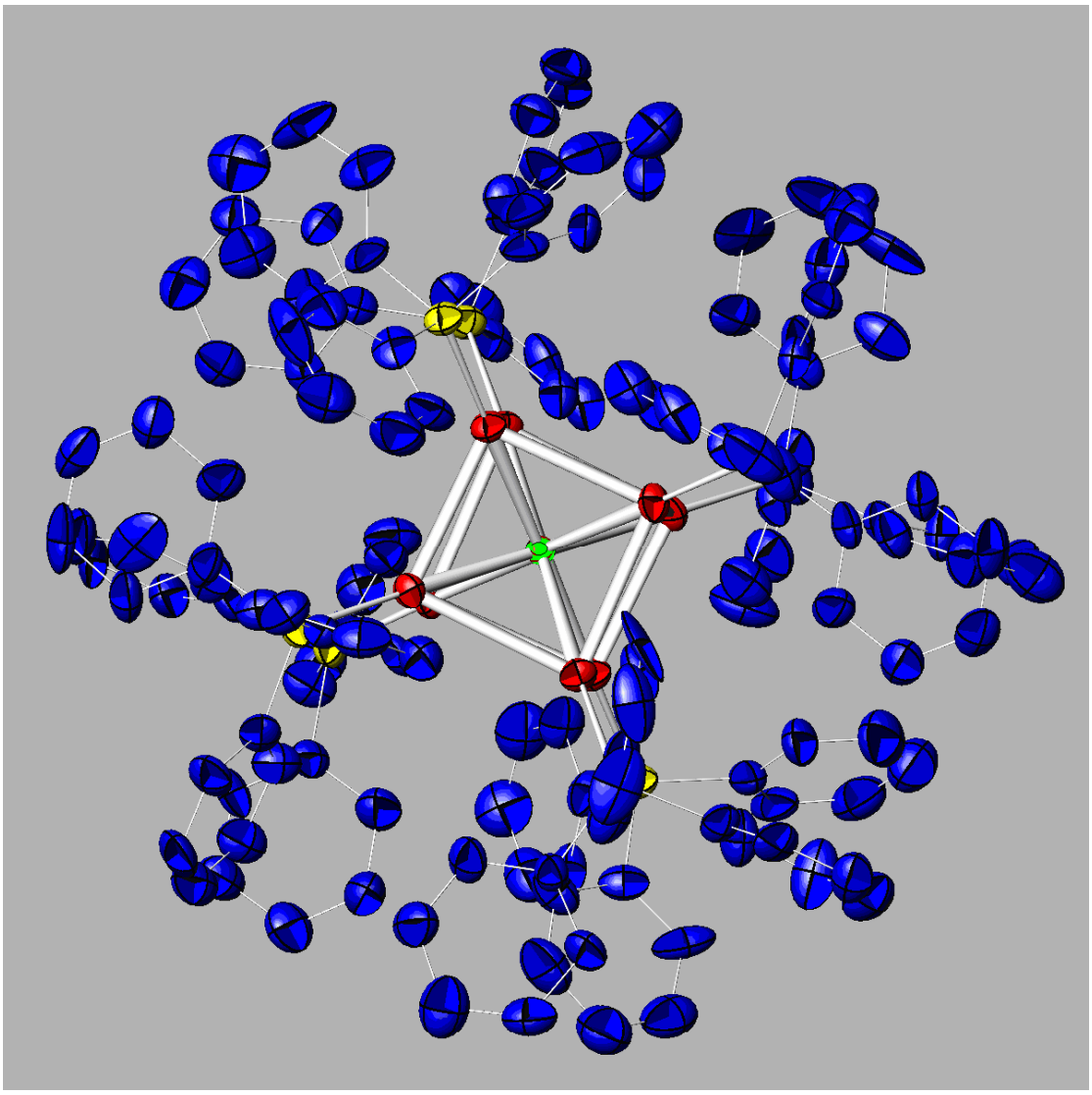

Figure 2.3. Drawing of the [Pb@Au_8] cluster showing the cubic structure. Pb is green, Au is red, P is yellow, and PPh_3 is blue.

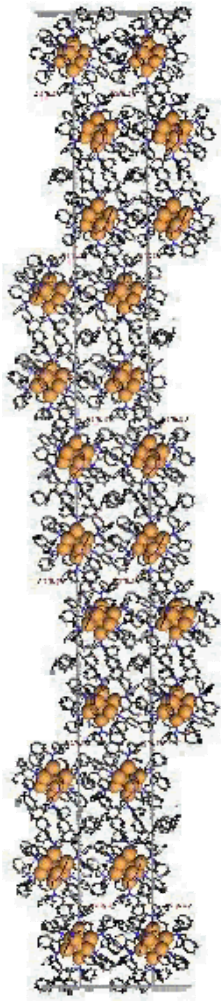

Figure 2.4. Unit cell of [Pb@Au_8] clusters (a,b = 16.5 Å, c = 184.6 Å).

Table 2.2. Crystallographic data for the [Pb@Au_8] complex

	$Pb(AuPPh_3)_8$
Empirical formula	$C_{162}H_{137}ClOP_9PbAu_8$
Formula weight	4181.81
Temperature (K)	213(2)
Wavelength (Å)	0.71073
Crystal system	Trigonal
Space group	R-3C
Unit cell dimensions	
a(Å)	16.5(10)
b(Å)	16.5(10)
c(Å)	184.588
α(deg)	90
ß(deg)	90
γ(deg)	120
Volume ($Å^3$)	43568(3732)
Z	12
Dcalc(Mg/m^3)	1.913
Abs coeff(mu)	8.997
Reflections collected	10571
Independent reflections	6707
	[R(int) = 0.0570]

Table 2.3. Selected bond lengths [Å] for [Pb@Au_8]

	Bond lengths (Å)
Pb-Au(1)	2.6031(7)
Pb-Au(2)	2.6074(7)
Pb-Au(3)	2.62(14)
Pb-Au(4)	2.61(14)
Au(1)-Au(3)	2.98(12)
Au(2)-Au(4)	2.93(12)
Au(3)-Au(4)	3.08(12)
Au(4)-Au(3)	3.08(12)
Au(1)-P(1)	2.273(4)
Au(2)-P(2)	2.268(4)
Au(3)-P(3)	2.30(12)
Au(4)-P(4)	2.29(12)
Cl(1)-P(9)	1.74(3)

Table 2.4. Selected bond angles [^{o}] for [Pb@Au_8]

	Bond angles (^{o})
$(Au\text{-}Pb\text{-}Au)_{avg}$	179.38(2)
	109.43(12)
	70.00(12)
$(Au\text{-}Au\text{-}Au)_{avg}$	89.67(2)
Pb(1)-Au(1)-Au(3)	55.5(16)
P(1)-Au(1)-Pb(1)	180.0
P(1)-Au(1)-Au(3)	124.5(16)

Table 2.5. Unit cell dimensions of some Pb clusters

Compound	S. Group	a(Å)	b(Å)	c(Å)	α(deg)	ß(deg)	γ(deg)
K_4Pb_9	P21/m	9.648(3)	13.243(5)	15.909(8)		103.24(4)	
$[K\text{-crypt}]_3Pb_9.0.5en$	P1-	14.962(5)	16.338(5)	20.48(1)	92.66(3)	96.37(3)	112.02(3)
$[K\text{-crypt}]_6Pb_9.1.5en.0.5tol$	P21/c	28.356(8)	23.757(5)	27.885(8)		94.01(2)	
$K^+[2,2,2\text{-crypt}K^+]_3Pb_9^{4-}$	P1-	15.811(1)	16.173(5)	20.180(6)	98.60(3)	104.59(2)	118.32(2)
$[Pb_{12}Pt][K\text{-crypt}]_2$	P-3	13.041(6)	13.041(6)	11.67(11)	90	90	120
$[K\text{-crypt}]_2Pb_5$	P3c1	11.702(3)	11.702(3)	22.124(9)	90	90	120
$[Pb@Au_8(PPh_3)_8]$	R-3c	16.5(10)	16.5(10)	184.58(8)	90	90	120

2.2.3 XPS Spectroscopic Studies

Since each element has a unique set of binding energies, X-ray photoelectron spectroscopy could be used to identify the elements on this Pb-Au cluster. XPS data are summarized in table 2.6. From the XPS spectra (Figure 2.5), elements Pb, Au, K, and Cl definitely exist in the cluster, which is consistent with the XRD results. Meanwhile, no Pt signal was found.

For Pb-Au cluster, we also tried EDX, NMR and ESI-MS to characterize it. From EDX results (see Appendix A), we couldn't find Pb atom in the cluster. This might be due to X-ray absorbed by Pb and another reason could be that Pb atom is in the center of the cubic cage, which makes it much more difficult to detect Pb. From NMR studies (see Appendix B), we didn't get the Pb-P coupling signal that was expected. We suspect some impurity existed in the solution. From ESI-MS studies (see Appendix C), we got really

complicated spectrum, especially for the negative mode. Pb(AuPPh3)8 signals were hard to figure out. These studies need further analysis in the future.

Table 2.6. XPS data of $Pb(AuPPh_3)_8$

Peak	**Position BE (eV)**	**FWHM (eV)**	**Raw Area (CPS)**	**RSF**	**Atomic Mass**	**Atomic Conc %**	**Mass Conc %**
Au 4f 7/2	85.251	1.899	11048.8	6.846	196.967	17.45	38.31
Au 4f 5/2	88.933	1.999	9011	6.846	196.967	14.22	31.21
Pb 4f 7/2	139.473	2.133	458.4	9.075	207.206	0.54	1.24
Pb 4f 5/2	144.585	2.359	354.7	9.075	207.206	0.42	0.96
Cl 2p a	199.28	2.463	1292.1	0.964	35.460	14.06	5.56
Cl 2p b	201.277	2.889	1185.4	0.964	35.460	12.89	5.1
K 2s	379.759	4.406	1727.6	0.422	39.102	40.42	17.62

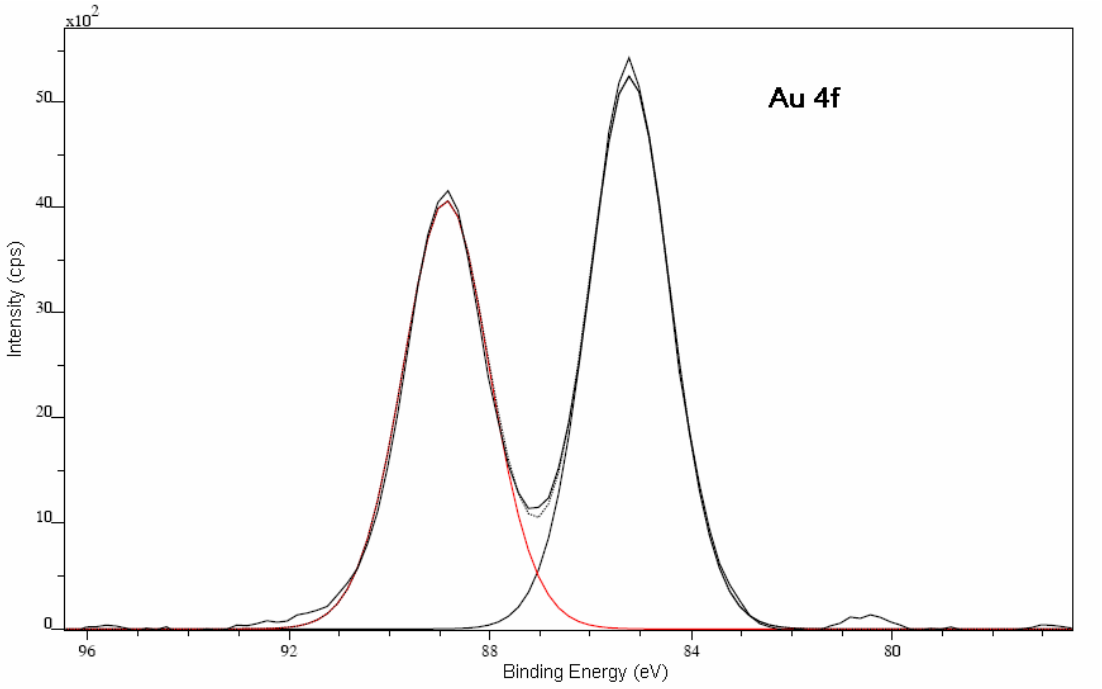
x10^2
Au 4f
Intensity (cps)
50
40
30
20
10
0
96
92
88
84
80
Binding Energy (eV)

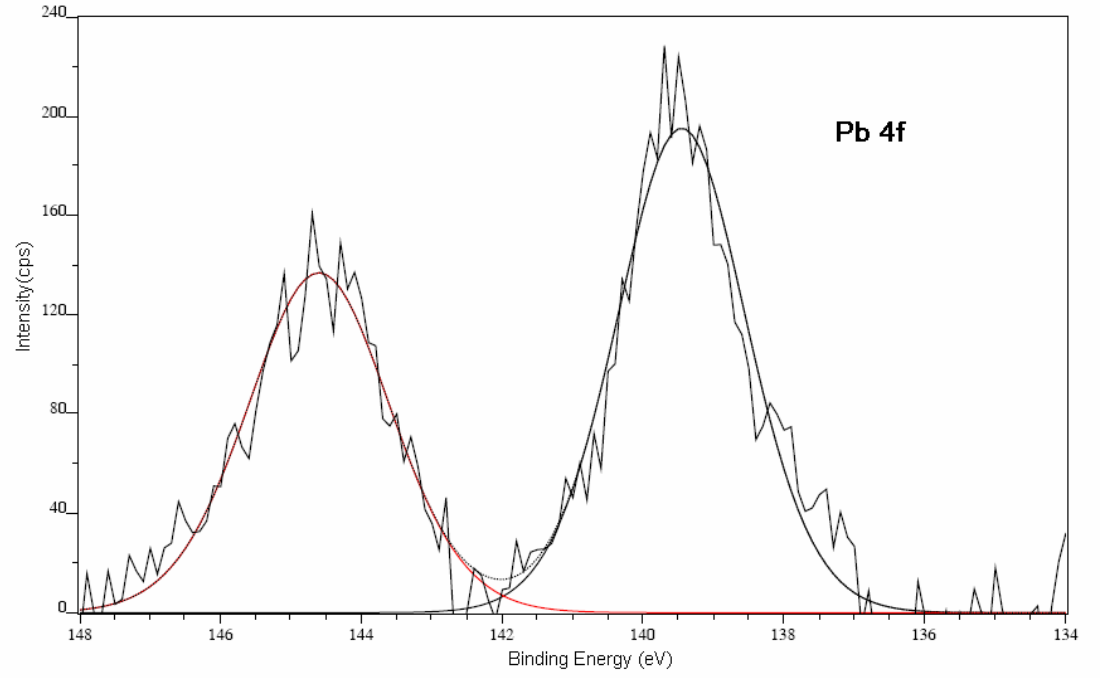
Pb 4f
Intensity (cps)
240
200
160
120
80
40
0
148
146
144
142
140
138
136
134
Binding Energy (eV)

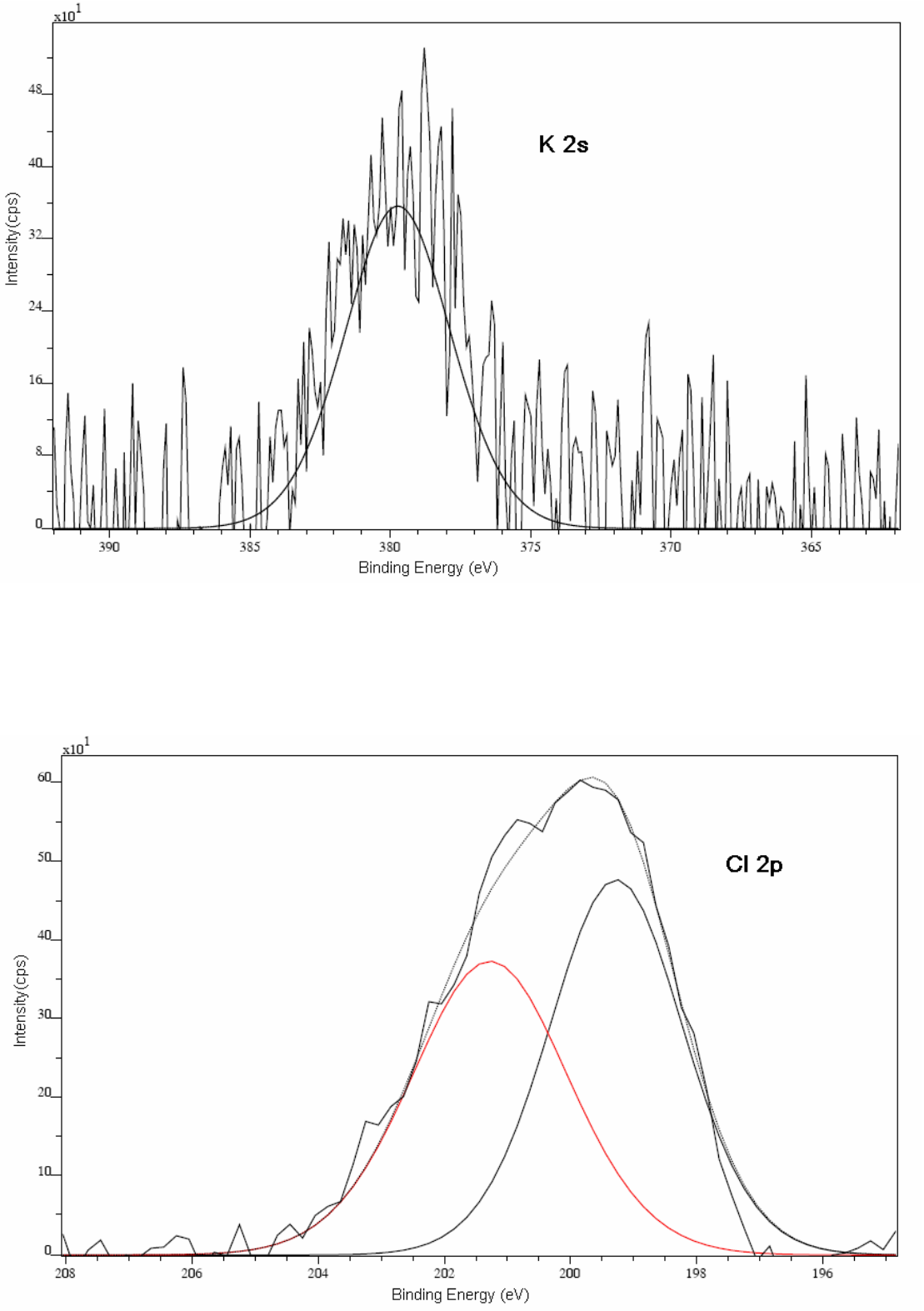

Fig 2.5. XPS spectrum of $Pb(AuPPh_3)_8$

2.3. Conclusion

A new Pb-Au complex has been isolated in this study. The [Pb@Au_8] cluster has intriguing highly symmetric, O_h structure. Similar 8 -Au atom, transition metal centered clusters have been reported, such as $M(AuPPh_3)_8^{2+}$, M = Pd or Pt and $Au(AuPPh_3)_8^{3+}$. However, the [Pb@Au_8] is the first Pb-Au cluster with its highly symmetric framework and a nearly perfect cubic structure.

The existence of the Pb atom in the complex was verified by XPS spectroscopy. The centered Pb atom has an unusual cubic Au_8 coordination environment with Au-Au contacts of 2.99 Å, avg. The Au-Au-Au angles (89.7°, avg) and P(1)-Au(1)-Pb angles (180°, avg) demonstrate the cubic O_h structure given by Single Crystal X-ray (XRD) data.

2.4. Experimental Section

2.4.1. General Data

All reactions were performed in a nitrogen atmosphere drybox (Vacuum Atmosphere Co.). The XRD data were recorded on a Single Crystal Diffractometer - Bruker Smart 1000. The ^{207}Pb NMR spectrum was recorded on a Bruker DRX500 Advance spectrometer operating at 83.7 MHz. AMRAY 1820K scanning electron microscope with a potential of 20kV was used for energy dispersive X-ray (EDX) studies. X-ray Photoelectron Spectroscopy was recorded on a high sensitivity Kratos AXIS 165 Spectrometer.

2.4.2 Chemicals

Melts of nominal composition K_4Pb_9 was made by fusion (at high temperature) of stoichiometric ratios of the elements. The chemicals were sealed in evacuated, silica tubes and heated carefully with a natural gas/oxygen flame. 4,7,13,16,21,24-Hexaoxa-1,10-diazobicyclo[8,8,8]-hexacosane (2,2,2-crypt) were purchased from Aldrich. KBH_4 and PPh_3AuCl were purchased from Strem. Anhydrous ethylenediamine (en) and dimethylformamide (DMF) were purchased from Fisher, vacuum distilled from K_4Sn_9, and stored under dinitrogen. Toluene was distilled from sodium/benzophenone under dinitrogen and stored under dinitrogen.

2.4.3. Synthesis

2.4.3.1. Preparation of [Pb@Au_8]

In vial 1, K_4Pb_9 (50mg, 0.0247mmol) and 2,2,2-crypt (37.3mg, 0.099mmol) were dissolved in en (～2ml) and stirred for ～5min., yielding a dark green solution. In vial 2, PPh_3AuCl (122.2mg, 0.247mmol) was dissolved in en (～1ml) yielding a clear solution. First KBH_4 (13.3mg, 0.247mmol) was added in vial 1, then the solution from vial 2 was added drop wise to vial 1 and mixture was stirred ～2h, yielding a reddish brown solution. The solution was then filtered through tightly packed glass wool. After two days, red crystals of [Pb@Au_8] precipitated. XPS analysis on crystals showed presence of Pb, Au, K, Cl atoms.

2.4.3.2. Crystallographic Studies

The crystal structures of the complexes were determined in single crystal X-ray facility at Chemistry and Biochemistry Department, University of Maryland, by Dr. Peter Zavalij.

Chapter 3

$[Pb_5]^{2-}$

3.1. Introduction

Kummer and Diehl[97] isolated the first solid derivative of a Zintl anion in 1970, namely, $Na_4(en)_7Sn_9$ (en = ethylenediamine), and incompletely characterized it by X-ray crystallography. More recently, Corbett and co-workers[98] have used 2,2,2-crypt as a sequestering agent for the alkali metal cations in order to prevent electron transfer from the anions to the cations. The use of 2,2,2-crypt has allowed the isolation and X-ray structural characterization of a number of heteropolyatomic naked cluster anions of groups III and IV [Sn_8Tl^{3-}, Sn_9Tl^{3-}][25] and homopolyatomic naked cluster anions of group IV [Ge_9^{m-}(m = 2, 3, and 4), Ge_{10}^{2-}, Ge_4^{2-}, Sn_9^{m-} (m = 3, 4), Sn_5^{2-}, Sn_4^{2-}, and Pb_5^{2-}[99] and group V [Sb_4^{2-}, Bi_4^{2-}].

In 1977, attempts to isolate the $(2,2,2\text{-crypt-M})^+$ (M = K and/or Na) salt of the Pb_9^{4-} anion by Corbett and co-workers[99] resulted in the unexpected isolation of the trigonal bipyramidal Pb_5^{2-} anion (D_{3h} point symmetry) in $(2,2,2\text{-crypt-Na})_2Pb_5$, which was, until recently only structurally characterized by X-ray crystallography. They obtained these compounds from solutions of the corresponding NaE_x (E = Sn, Pb) precursors in en in the presence of crypt and characterized the first compounds $[Na\text{-}(2,2,2\text{-crypt})]_2Sn_5$ and $[Na\text{-}(2,2,2\text{-crypt})]_2Pb_5$ with the trigonal bipyramidal *closo*-$[E_5]^{2-}$ cluster anions (E = Sn, Pb). The Zintl phase derivative $[K\text{-}(2,2,2\text{-crypt})]_2Pb_5$ was prepared in a similar way, but it was not structurally characterized. Surpringly, although

the NMR characterization of the Pb_5^{2-} anion has been alluded to,[100] no unambiguous resonances in solution by ^{207}Pb NMR spectroscopy have been reported in the range from +2000 to -5500 ppm, the region where the ^{207}Pb resonances of lead clusters are normally expected to occur.[101-105] In comparison, the Pb_9^{4-} anion and its mixed analogs $Sn_{9-x}Pb_x^{4-}$ (x = 0-9), $Sn_{9-x}Ge_x^{4-}$ (x = 0-8), $Sn_{8-x}Pb_xTl^{5-}$ (x = 0-8) and Sn_8Tl^{5-} have been identified in en solutions by ^{207}Pb, ^{205}Tl and ^{119}Sn NMR spectroscopy.

Campbell and coworkers[106] stated that all solutions, whether containing a stoichiometric deficit or an excess of 2,2,2-crypt, gave rise to crystalline material having three distinct morphologies: dark red needle-shaped crystals, whose morphology resembled the morphologies previously described for $(2,2,2\text{-crypt-}K^+)_2Pb_5^{2-}$ and $(2,2,2\text{-crypt-}Na^+)_2Pb_5^{2-}$,[99] which failed to diffract, and hexagonal and parallelepiped shaped crystal morphologies whose unit cells were unknown. Subsequently, the latter crystals were characterized by X-ray crystallography and shown to be $K(2,2,2\text{-crypt-}K)_3Pb_9$ and $(2,2,2\text{-crypt-}K)_3Pb_9$, respectively, while they could not observe any NMR signals corresponding to the Pb_5^{2-} anion in either of these solutions.

The present work reports the preparation and the structural characterization of Pb_5 cluster anions in the salts $K^+(2,2,2\text{-crypt-}K^+)_2Pb_5^{2-}$. We found an exciting stable ^{207}Pb NMR signal for Pb_5^{2-}. Further discussion based on the population statistical calculations of cluster Pb_5^{2-} is presented.

3.2. Results and Discussion

3.2.1. Synthesis

Crystals of [K-(2,2,2-crypt)]$_2$Pb$_5$ were obtained as a precipitation product after the reaction of PPh$_3$AuCl with a solution of K$_4$Pb$_9$ in en in the presence of crypt. After one week at room temperature, a small quantity of long dark red trigonal crystals of [K-crypt]$_2$Pb$_5$ were formed on the glass wall close to the glass/liquid/gas phase boundary together with some shiny black prismatic 'crystals'. The powder of the black product turned out to be amorphous to X-rays.

3.2.2. Properties

Crystalline [K-(2,2,2-crypt)]$_2$Pb$_5$ is transparent dark red. The compound is sensitive to oxidation and hydrolysis and has to be handled under inert conditions (i.e. glove box).

3.2.3. Crystal Structure Determination

[K-(2,2,2-crypt)]$_2$Pb$_5$ is isotructural with [Na-(2,2,2-crypt)]$_2$Pb$_5$.[99] The structure is characterized by isolated $[Pb_5]^{2-}$ Zintl anions, which are well separated from each other by the $[K^+$-(2,2,2-crypt)] inclusion complexes. (Figure 3.1)

The X-ray diffraction data of a single crystal of [K-(2,2,2-crypt)]$_2$Pb$_5$ were recorded using a Bruker Smart 1000 Single Crystal Diffractometer. The unit cell dimensions were determined from the least-square refinement of the 2θ values of 29 reflections ($15.5^o \leqslant 2\theta \leqslant 24.8^o$). The Laue symmetry, the systematic reflection absences and the $|E|$ distribution lead to the trigonal space group $P\bar{3}c1$. These data indicated that the compound is isotypic with [Na-(2,2,2-crypt)]$_2$Pb$_5$.[99] The positional parameters of

[Na-(2,2,2-crypt)]$_2$Pb$_5$ were used as starting set for the structure refinement. The refinement on the whole F^2 data converged rapidly. Summaries of the crystallographic data and selected bond distances and angles for the clusters are given in Table 3.1 and Table 3.2.

Table 3.1. Crystallographic data for [K-(2,2,2-crypt)]$_2$Pb$_5$.

Crystal	Black trigonal prism	
Crystal size	0.49 × 0.24 × 0.22 mm^3	
Space group	P $\bar{3}$c1	
Empirical formula	C36 H72 K2 N4 O12 Pb5	
Formula weight	1867.13	
Temperature	213(2) K	
Wavelength	0.71073 Å	
Crystal system	Trigonal	
Unit cell dimensions	a = 11.7024(3) Å	α = 90°
	b = 11.7024(3) Å	β = 90°
	c = 22.1247(9) Å	γ = 120°
Volume	2623.96(14) Å^3	
Z	2	
Density, ρ_{calc}	2.363 g/cm^3	
Absorption coefficient, μ	16.199 mm^{-1}	
F(000)	1720 $\bar{e}$	

Table 3.2. Selected Bond lengths (Å) and angles (°) for $[K\text{-}(2,2,2\text{-crypt})]_2Pb_5$. Standard deviations are given in parentheses.

Pb1-Pb2	3.0090(5)
Pb1-Pb1	3.2575(6)
Pb2-Pb1	3.0090(5)
K1-O2	2.690(2)
K1-O1	2.784(3)
K1-N2	2.928(7)
K1-N1	2.974(7)
N1-C1	1.469(6)
C1-C2	1.517(8)
C2-O1	1.433(6)
O1-C3	1.428(6)
C3-C4	1.494(6)
C4-O2	1.4249
O2-C5	1.4178
C5-C6	1.513(5)
C6-N2	1.474(5)
Pb2-Pb1-Pb2	102.631(16)
Pb2-Pb1-Pb1	57.229(6)
Pb1-Pb1-Pb1	60.0
Pb1-Pb2-Pb1	65.543(13)

The Pb_5^{2-} anions have five Pb atoms that form an trigonal bipyramid (Figure 3.1a). The anions possess virtual molecular D_{3h} point symmetry. The Pb-Pb contacts (3.133 Å, ave) for the anions are in agreement with the ones reported from polyplumbide clusters $[Pb_9]^{4-}$[106] and $[Pb_5]^{2-}$[99], where the distances vary between 3.0090 Å and 3.2575 Å.

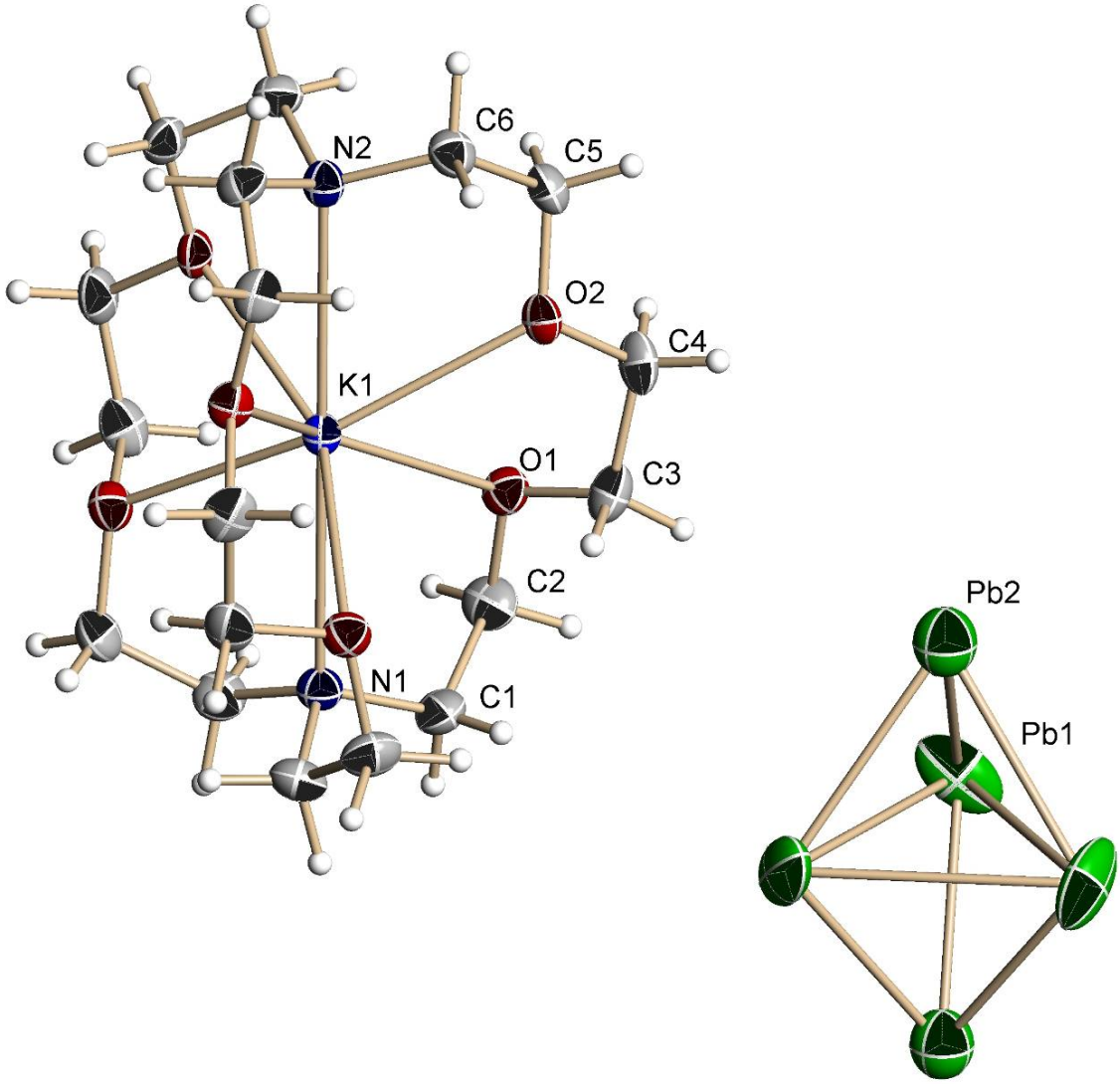

Figure 3.1. A view of a molecule of $[K(2,2,2\text{-crypt})]_2Pb_5$ from the crystal structure showing the numbering scheme employed. Anisotropic atomic displacement ellipsoids for the non-hydrogen atoms are shown at the 50% probability level. Hydrogen atoms are displayed with an arbitrarily small radius.

3.2.4. NMR Spectroscopic Studies

The ^{207}Pb NMR data of the $[Pb_5]^{2-}$ are summarized in Table 3.3.

Table 3.3. The ^{207}Pb NMR chemical shifts

Anions	**δ(ppm)**
$[Pb_5]^{2-}$	-3591
	-8600
$[Pb_9]^{4-}$	-4098
$[Ni@Pb_{10}]$	-996
$[Pt@Pb_{12}]^{2-}$	+1780
$[Pd@Pb_{12}]^{2-}$	+1520
$[Ni@Pb_{12}]^{2-}$	+1167

Naked lead anions have chemical shifts moved significantly upfield when they are compared to other lead clusters such as $[M@Pb_{12}]^{2-}$ (M = Pt, Pd, Ni) and $[Ni@Pb_{10}]^{2-}$.[45, 107] The ^{207}Pb NMR spectrum of the anion shows a singlet at -3591 ppm flanked by Pb satellites ($^1J_{^{207}Pb\text{-}^{207}Pb} \approx$ 2344 Hz, at -45 ^oC and -15 ^oC, 83.7 MHz) indicating strong coupling between two kinds of Pb atoms.(Figure 3.2a) In comparison, Pb_9^{4-} shows a relatively sharp resonance at -4098 ppm ($\Delta \nu_{1/2}$ = 47 Hz, at 25^oC, 104.7 MHz) as a result of fast exchange on the NMR time Scale.[106]

We also did the population statistical calculation for $[Pb_5]^{2-}$ anions (table 3.4). Based on the five case analysis of Pb1&Pb2 combinations, we expect two ^{207}Pb NMR signals for Pb_5^{2-} anions, one is Pb1 centered with Pb2 doublet lines with the ratio around 4:1, and

the other is Pb2 centered with Pb1 doublet lines with the ratio around 3:1. The signal at -3591 ppm is well consistent with the 4:1 ratio. Another singlet at around -8600 ppm (Figure 3.2b) seems not to be the other one we expected. We are still trying to find the other signal, which might be in a much broader range.

(a)

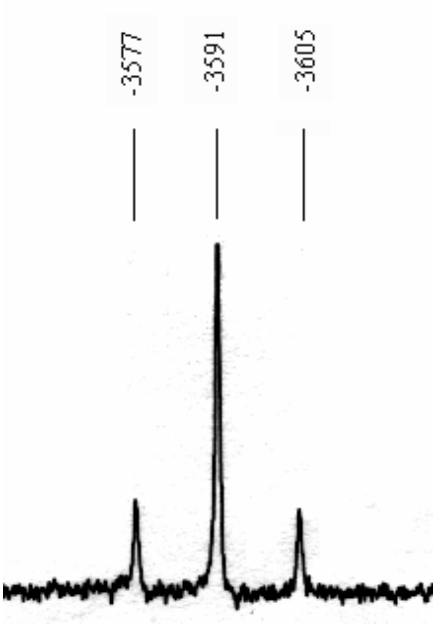

(b)

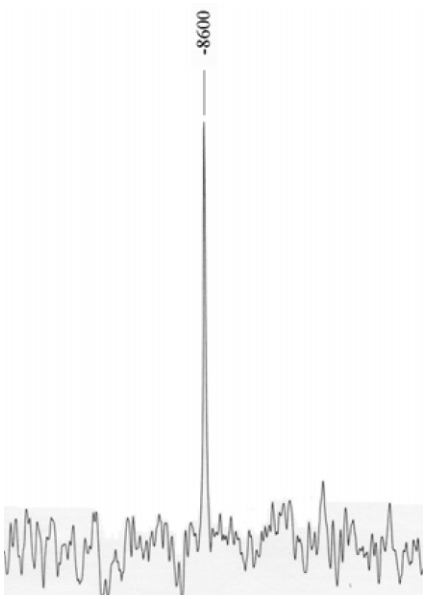

Figure3.2. The ^{207}Pb NMR Spectrum of $[Pb_5]^{2-}$ ion recorded in dmf (a) @ -45^{o}C, -15 ^{o}C and 83.7MHz; (b) @ -15 ^{o}C and 83.7MHz.

3.3. Conclusion

The $[Pb_5]^{2-}$ anion described here is very intriguing with its surprising NMR resonances. The low temperature ^{207}Pb NMR spectrum of $[Pb_5]^{2-}$ at -45°C and -15°C contains a singlet at -3591ppm flanked by Pb satellites ($^1J_{^{207}Pb-^{207}Pb} \approx$ 2344 Hz, at -45 °C and -15 °C, 83.7 MHz). The intensity ratio is 1:4:1, which is in well agreement with its D_{3h} structure under two different Pb environments.

The ^{207}Pb NMR analysis also gives important knowledge about dynamic behavior of the cluster anions described here. At low temperature, the $[Pb_5]^{2-}$ anion showed no intramolecular exchange of the two kinds of Pb atoms. Upon increasing the temperature from -45°C to -15°C, the line widths of the peaks remain the same. This revealed that the spectra are consistent with solid state structure of the compound, and it is static on NMR time scale in comparison with the fluxional nature of the anion Pb_9^{4-}.

3.4. Experimental Section

3.4.1. General Data

All reactions were performed in a nitrogen atmosphere drybox (Vacuum Atmosphere Co.). The ^{207}Pb NMR spectrum was recorded on a Bruker DRX500 Advance spectrometer operating at 83.7 MHz.

3.4.2 Chemicals

Melts of nominal composition K_4Pb_9 was made by fusion (at high temperature) of stoichiometric ratios of the elements. The chemicals were sealed in evacuated, silica tubes and heated carefully with a natural gas/oxygen flame. 4,7,13,16,21,24-Hexaoxa-

1,10-diazobicyclo[8,8,8]-hexacosane (2,2,2-crypt) were purchased from Aldrich. PPh_3AuCl were purchased from Strem. Anhydrous ethylenediamine (en) and dimethylformamide (DMF) were purchased from Fisher, vacuum distilled from K_4Sn_9, and stored under dinitrogen. Toluene was distilled from sodium/benzophenone under dinitrogen and stored under dinitrogen.

3.4.3. Synthesis

3.4.3.1. Preparation of [K(2,2,2-crypt)]Pb5

In vial 1, K_4Pb_9 (80mg, 0.0395mmol) and 2,2,2-crypt (59.6mg, 0.158mmol) were dissolved in en (～2ml) and stirred for ～5min., yielding a dark green solution. In vial 2, PPh_3AuCl (15mg, 0.0303mmol) was dissolved in en (～1ml) yielding a clear solution. The solution in vial 2 was added drop wise to vial 1 and mixture was stirred ～2h. yielding a dark red solution. The solution was then filtered through tightly packed glass wool. After two days, dark red crystals of [K(2,2,2-crypt)]Pb_5 precipitated.

3.4.3.2. Crystallographic Studies

The crystal structures of the complexes were determined at single crystal X-ray facility at Chemistry and Biochemistry Department, University of Maryland, by Dr. Peter Zavalij.

Table 3.4. Population Statistical Calculation for $[Pb_5]^{2-}$ anion

$[Pb_5]^{2-}$ (Trigonal bipyramid: 3Pb1(A) and 2Pb2(B))

	^{207}Pb	^{X}Pb		
Natural abundance	22.10%	77.90%		
	Atom numbers		Population statistical results	^{207}Pb NMR results
Case 0	0	5	(0.779)5 =0.28687	silent
Case 1	1	4	1 on B: 2*(0.221)*(0.779)4 = 0.16277	B Singlet
			1 on A: 3*(0.221)*(0.779)4 = 0.24415	A singlet
Case 2	2	3	2 on B: (0.221)2 * (0.779)3 = 0.02309	B Singlet
			2 on A: 3*(0.221)2 * (0.779)3 = 0.06926	A singlet
			1 on B and 1 on A: 2*(0.221) 3*(0.221) (0.779)3 = 0.13853	AB doublet for both A and B
Case 3	3	2	3 on A: (0.221)3 (0.779)2 = 0.00655	A singlet
			2 on B and 1 on A: [(0.221)2] 3*(0.221) (0.779)2 = 0.01965	AB_2 triplet for A or BA doublet for B
			2 on A and 1 on B: [3*(0.221)2] [2*(0.221)] (0.779)2 = 0.03930	BA_2 triplet for B or AB doublet for A
Case 4	4	1	1 on B and 3 on A: 2*(0.221) (0.221)3 (0.779) = 0.00372	BA_3 quantet for B or AB doublet for A
			2 on B and 2 on A: [(0.221)2][3*(0.221)2] (0.779) = 0.00558	BA_2 triplet for B or AB_2 triplet for A
Case 5	5	0	2 on B and 3 on A: (0.221)5 = 0.00053	BA_3 quantet for B or AB_2 triplet for A
Sum			1	
B central line / doublet line			(0.16277+0.02309+0.03930+0.00558) / [(0.13853+0.01965)/2] = 2.92	
A central line / doublet line			(0.24415+0.06926+0.00655+0.01965+0.00558+0.00053) / [(0.13853+0.03930+0.00372)/2] = 3.81	

Appendix A: EDX Spectrum and data

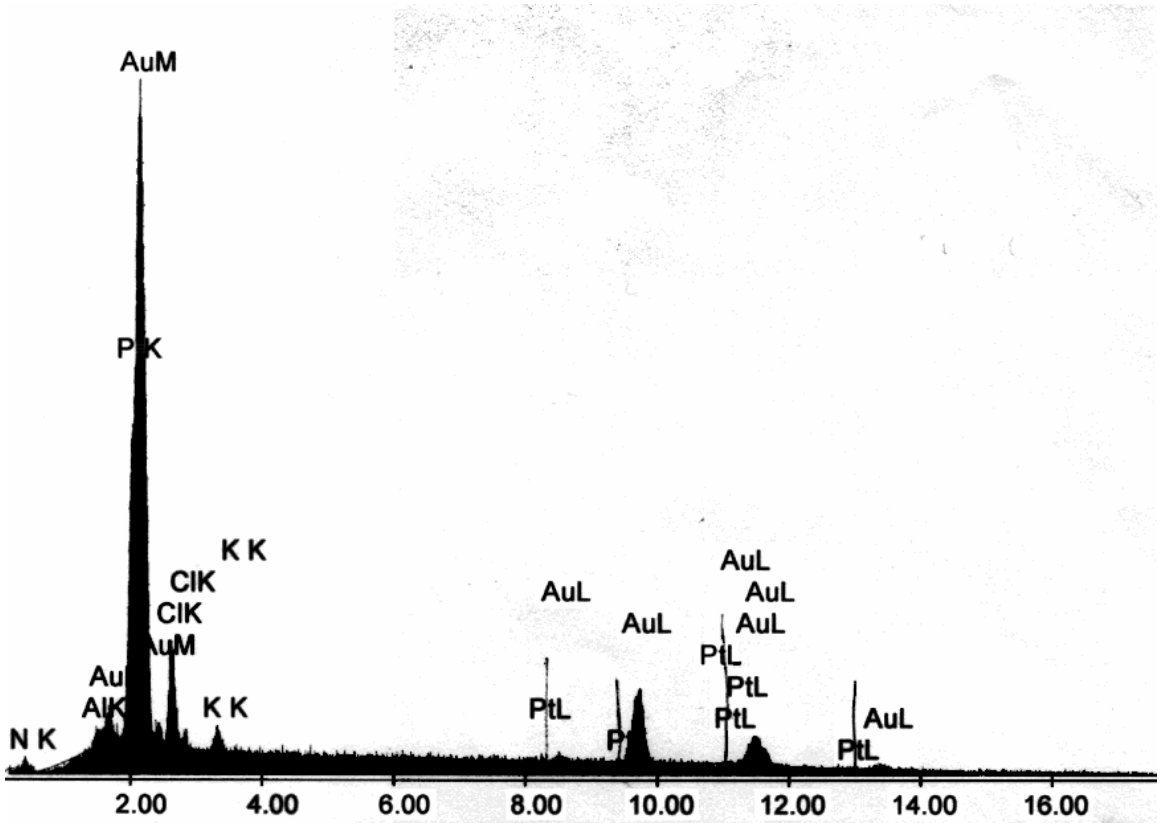

The EDX Spectrum of Pb-Au complex recorded @ 20°C

Element	Wt%	At%	K-Radio	Z	A	F
N K	2.40	14.49	0.0036	1.2890	0.1150	1.0000
Al K	0.97	3.04	0.0045	1.1844	0.3867	1.0024
P K	9.81	26.78	0.0710	1.2252	0.5903	1.0016
Cl K	7.85	18.74	0.0306	1.2146	0.3207	1.0004
K K	1.73	3.75	0.0081	1.1896	0.3909	1.0000
Pt L	2.41	1.05	0.0217	0.8880	1.0116	1.0000
Au L	74.82	32.14	0.6733	0.8879	1.0135	1.0000
Total	100.00	100.00				

Element	Net Inte.	Bkgd Inte.	Inte. Error	P/B
N K	2.58	0.67	6.99	3.85
Al K	5.45	7.39	6.57	0.74
P K	76.57	8.47	1.20	9.04
Au M	187.71	9.24	0.75	20.31
Cl K	29.79	9.00	2.09	3.31
K K	6.73	8.23	5.75	0.82
Pt L	1.17	6.48	23.73	0.18
Au L	32.54	6.40	1.92	5.08

Appendix B: NMR Spectrum

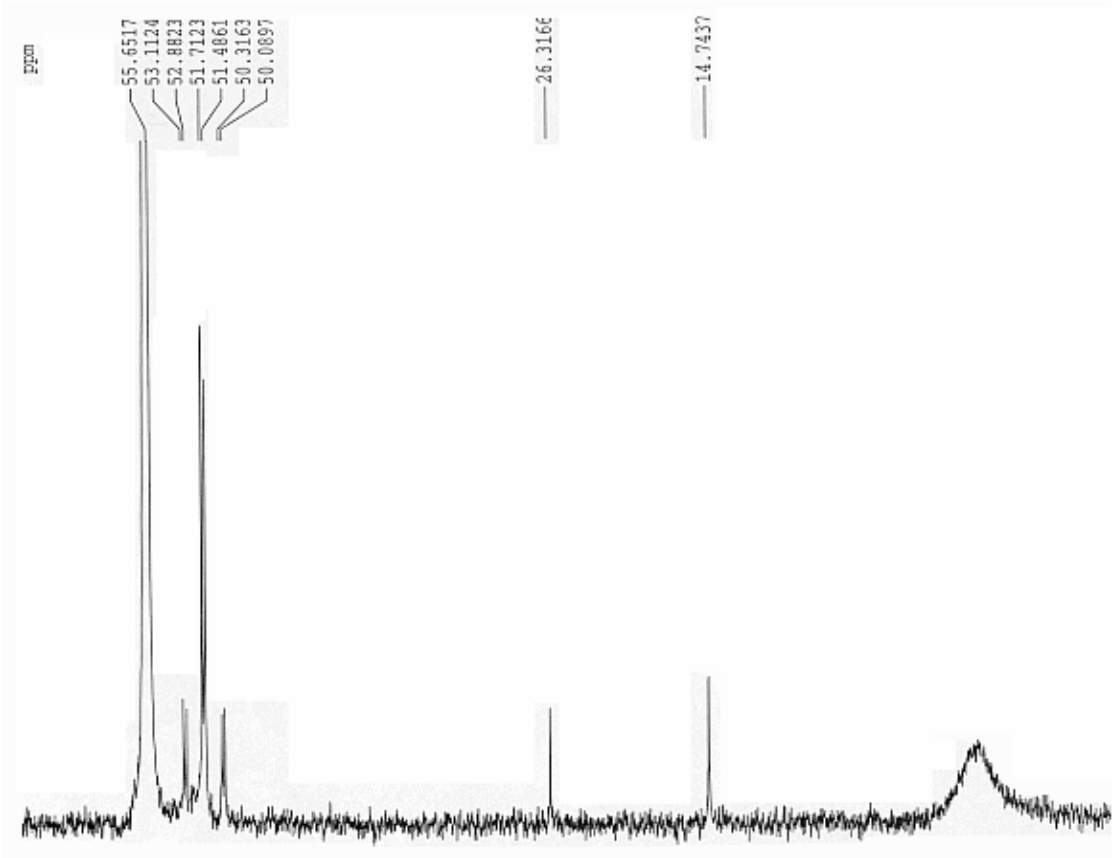

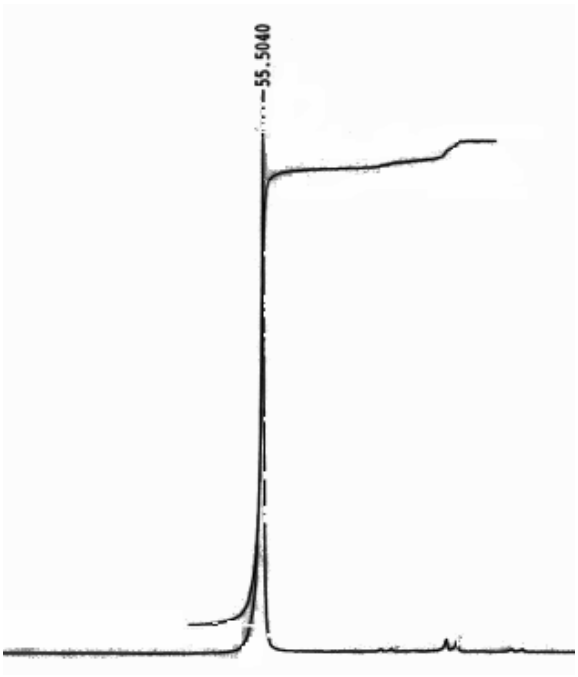

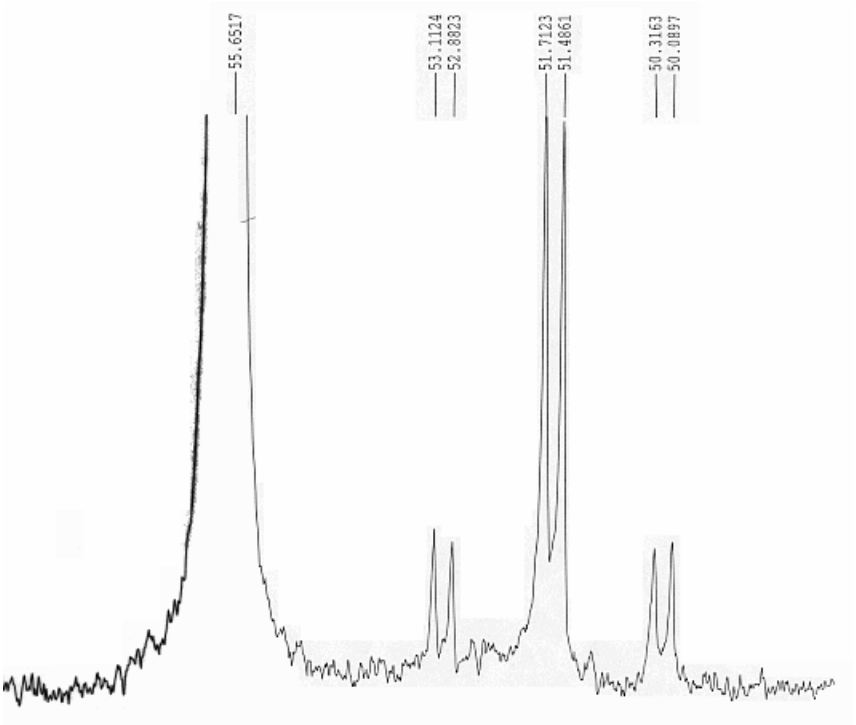

The ^{31}P NMR(decoupled) Spectrum of Pb-Au complex recorded in dmf @ 15 ^{o}C and 161.98 MHz.

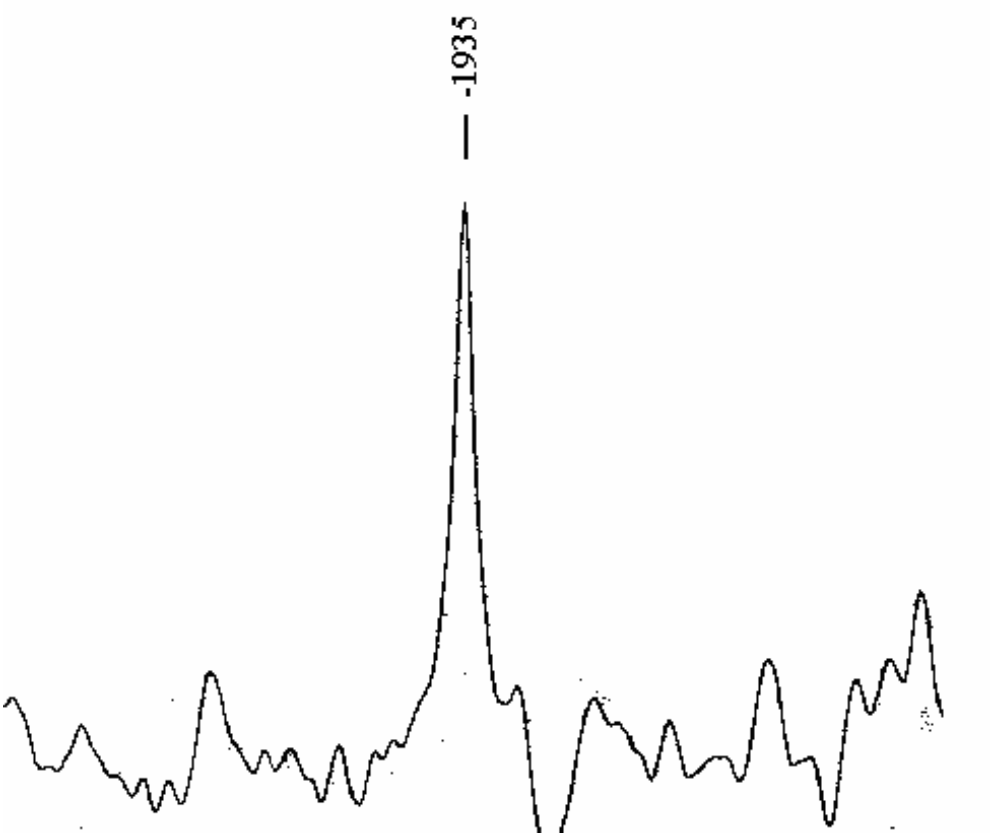

The ^{207}Pb NMR Spectrum of Pb-Au complex recorded in dmf @ 16 ^{o}C and 83.6 MHz.

Appendix C: ESI-MS Spectrum

(a)

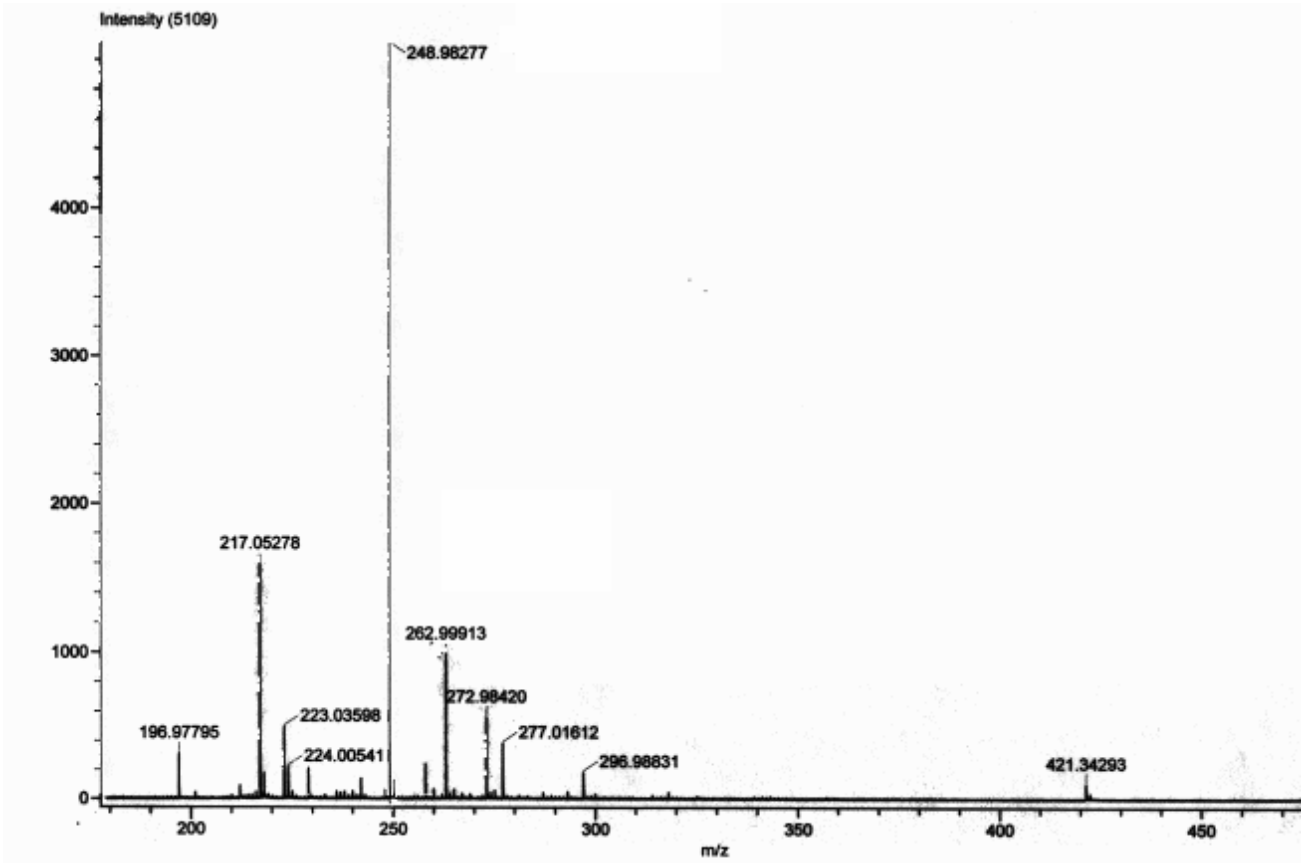

(b)

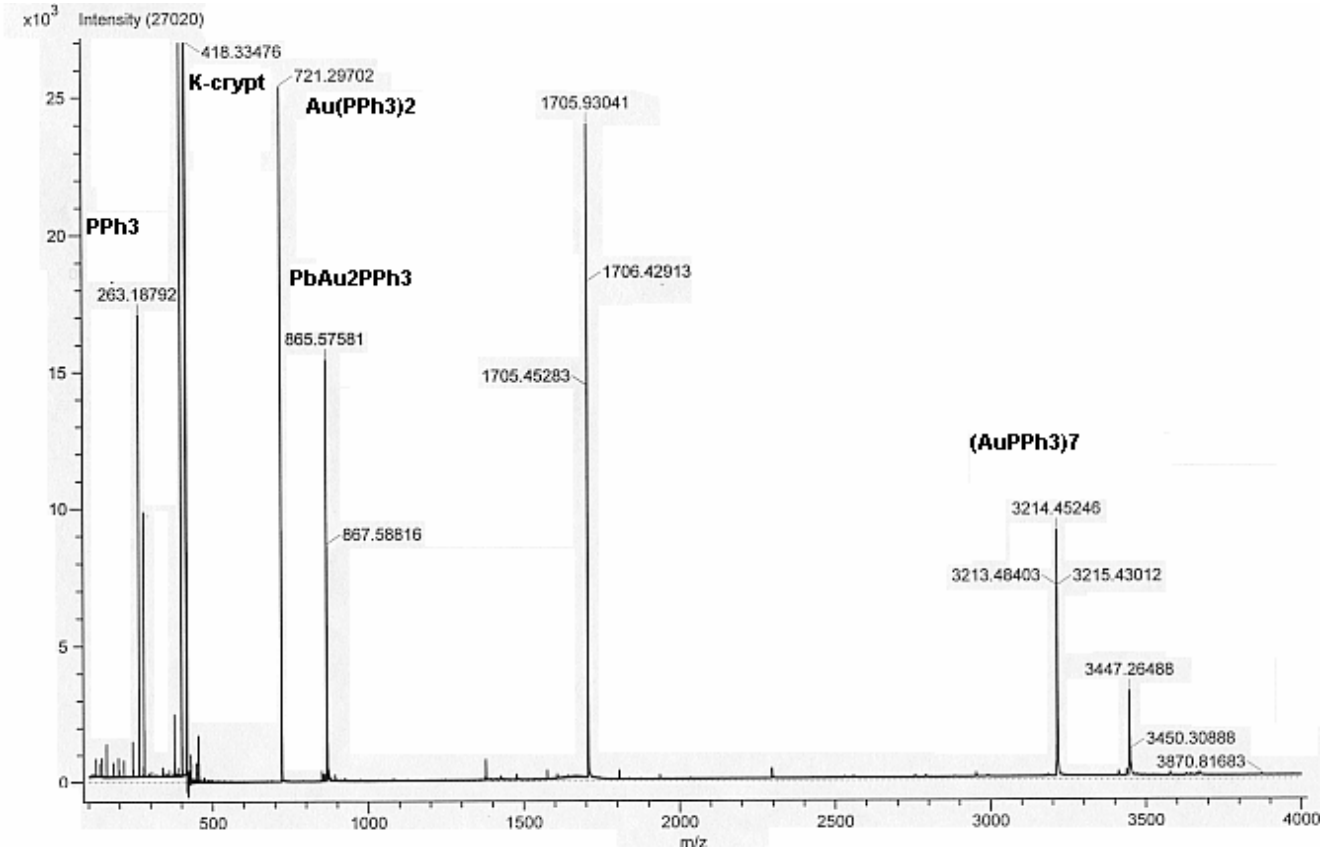

The ESI-MS Spectrum of Pb-Au complex recorded in dmf @ 20 ^{o}C, (a) negative mode (b) positive mode.

References

[1] A. C. Muller, P. A. Engelhard, J. E. Weisang, *Journal of Catalysis* **1979**, *56*, 64.

[2] S. G. Fiddy, M. A. Newton, T. Campbell, J. M. Corker, A. J. Dent, I. Harvey, G. Salvini, S. Turin, J. Evans, *Chemical Communications* **2001**, 445.

[3] Z. Huang, J. R. Fryer, C. Park, D. Stirling, G. Webb, *Journal of Catalysis* **1998**, *175*, 226.

[4] R. Pool, *Science* **1990**, *248*, 1186.

[5] G. Schmid, *Clusters and Colloids*, VCH, Weinheim, **1994**.

[6] M. N. Vargaftik, V. P. Zargorodnikov, I. P. Stolarov, I. I. Moiseev, D. I. Kochubey, V. A. Likholobov, A. L. Chuvilin, K. I. Zamaraev, *J. Mol. Catal.* **1989**, *53*, 315.

[7] D. E. Bergeron, A. W. Castleman, T. Morisato, S. N. Khanna, *Science* **2004**, *304*, 84.

[8] K. H. Bowen, *Personal communication*.

[9] A. Ecker, E. Weckert, H. Schnonkel, *Nature* **1997**, *387*, 379.

[10] S. Neukermans, E. Janssens, Z. F. Chen, R. E. Silverans, P. V. Schleyer, P. Lievens, *Physical Review Letters* **2004**, 92.

[11] B. Kesanli, *Ph. D, Dissertation*, **2002**.

[12] M. Moses, J. Fettinger, B. Eichhorn, *Science* **2003**, *300*, 778.

[13] A. Joannis, **1891**, *113*, 795.

[14] A. Joannis, **1892**, *114*, 585.

[15] C. A. Kraus, *Journal of the American Chemical Society* **1907**, *29*, 1557.

[16] C. A. Kraus, *Journal of the American Chemical Society* **1922**, *44*, 1216.

[17] F. H. Smyth, *Journal of the American Chemical Society* **1917**, *39*, 1299.

[18] L. Diehl, K. Khodadadeh, D. Kummer, *J. Chem. Ber* **1976**, *109*, 3404.

[19] D. G. Adolphson, J. D. Corbett, D. J. Merryman, *Journal of the American Chemical Society* **1976**, *98*, 7234.

[20] T. F. Fassler, R. Hoffmann, *Angewandte Chemie-International Edition* **1999**, *38*, 543.

[21] J. D. Corbett, P. A. Edwards, *Journal of the American chemical Society* **1977**, *99*, 3313.

[22] T. F. Fassler, R. Hoffmann, *J. Chem. Soc.- Dalton. Trans.* **1999**, 3339.

[23] E. Todorov, S. C. Sevov, *Inorganic Chemistry* **1998**, *37*, 3889.

[24] V. Queneau, S. C. Sevov, *Angewandte Chemie-International Edition* **1997**, *36*, 1754.

[25] C. H. E. Belin, J. D. Corbett, A. Cisar, *Journal of the American Chemical Society* **1977**, *99*, 7163.

[26] W. Dahlmann, H. G. ConSchnering, *Naturwissenschaften* **1973**, *60*, 429.

[27] W. Dahlmann, Vschneri. Hg, *Naturwissenschaften* **1972**, *59*, 420.

[28] F. Laves, *Naturwissenschaften* **1941**, *29*, 244.

[29] S. C. Critchlow, J. D. Corbett, *Inorganic Chemistry* **1984**, 23.

[30] B. W. Eichhorn, R. C. Haushalter, *Journal of the Chemical Society. Chemical Communications* **1990**, 937.

[31] E. B. Campbell, g. J. Schrobilgen, *Inorganic Chemistry* **1997**, *36*, 4078.

[32] S. C. Critchlow, J. D. Corbett, *Journal of the American Chemical Society* **1983**, *105*, 5715.

[33] T. F. Fassler, M. Hunziker, *Inorganic Chemistry* **1994**, *33*, 5380.

[34] T. F. Fassler, U. Schutz, *Inorganic Chemistry* **1999**, *38*, 1866.

[35] T. F. Fassler, *Coordination Chemistry Reviews* **2001**, *215*, 347.

[36] J. D. Corbett, P. A. Edwards, *Journal of the American Chemical Society* **1977**, *99*, 3313.

[37] J. D. Corbett, *Chemical Reviews* **1985**, *85*, 383.

[38] K. Wade, *Adv. Inorg. Chem. Radichem* **1976**, *18*, 1.

[39] B. W. Eichhorn, R. C. Haushalter, W. T. Pennington, *Journal of the American Chemical Society* **1988**, *110*, 8704.

[40] B. Kesanli, J. Fettinger, B. Eichhorn, *Chemistry-a European Journal* **2001**, *7*, 5277.

[41] B. Kesanli, J. Fettinger, D. R. Gardner, B. Eichhorn, *Journal of the American Chemical Society* **2002**, *124*, 4779.

[42] B. Schiemenz, G. Huttner, *Angewandte Chemie-International Edition in English* **1993**, *32*, 297.

[43] G. Renner, P. Kircher, G. Huttner, P. Rutsch, K. Heinze, *European Journal of Inorganic Chemistry* **2001**, 973.

[44] S. M. Kauzlarich, *Chemistry, Structure and Bonding of Zintl Phases and Ions*, VCH Publishers Inc., New York, **1996**.

[45] E. N. Esenturk, J. Fettinger, Y.-F. Lam, B. Eichhorn, *Angew. Chem*. **2004**, *116*, 2184; *Angew. Chem. Int. Ed*. 2004, *43*, 2132.

[46] J. M. Goicoechea, S. C. Sevov, *Journal of the American Chemical Society* **2005**, *127*, 7676.

[47] J. M. Goicoechea, S. C. Sevov, *Angewandte Chemie-International Edition* **2005**, *44*, 4026.

[48] M. Haruta, *Catal. Today* **1997**, *36*, 153, and references therein.

[49] For a recent highlight on nanogold, see P. Schwerdtfeger, *Angew. Chem., Int. Ed.* **2003**, *42*, 1892.

[50] P. Pyykko, *Chem. Rev. (Washington, D. C.)* **1988**, *88*, 563.

[51] H. Schmidbaur, *Gold Bull. (Lindon)* **2000**, *33*, 3.

[52] J. Li, X. Li, H. J. Zhai, and L. S. Wang, *Science* **2003**, *299*, 864.

[53] H. F. Zhang, M. Stender, R. Zhang, C. Wang, J. Li, and L. S. Wang, *J. Phys. Chem. B* **2004**, *108*, 12259.

[54] M. P. Johansson, D. Sundholm, and J. Vaara, *Angew. Chem., Int. Ed.* **2004**, *43*, 2678.

[55] X. Gu, M. Ji, S. H. Wei, and X. G. Gong, *Phys. Rev. B* (in press).

[56] F. Furche, R. Ahlrichs, P. Weis, C. Jacob, T. Bierweiler, and M. Kapppes, *J. Chem. Phys.* **2002**, *117*, 6982.

[57] P. Pyykko, N. Runeberg, *Angewandte Chemie-International Edition* **2002**, *41*, 2174.

[58] D. M. P. Mingos, *J. Chem. Soc. Dalton Trans.* **1976**, 1163.

[59] C. E. Briant, B. R. C. Theobald, J. W. White, L. K. Bell, D. M. P. Mingos, and A. J. Welch, *J. Chem. Soc., Chem. Commun.* **1981**, 201.

[60] X. Li, B. Kiran, J. Li, H. Zhai, L. Wang, *Angewandte Chemie-International Edition* **2002**, *41*, 4786.

[61] H. Zhai, J. Li, L. Wang, **2004**, *121*, 8369.

[62] G. Schmid, R. Pfeil, R. Boese, F. Bandermann, S. Meyer, g. H. M. Calis, *J. W. A. Chem. Ber.* **1981**, *114*, 3634.

[63] R. Prasada, *Advances in Catalysis Science and Technology*, Halsted Press, **1985**.

[64] M. M. Schubert, M. J. Kahlich, G. Feldmeyer, M. Huttner, S. Hackenberg, H. A. Gasteiger, R. J. Behm, *Physical Chemistry Chemical Physics* **2001**, *3*, 1123.

[65] Y. Morimoto, E. B. Yeager, *Journal of Electroanalytical Chemistry* **1998**, *441*, 77.

[66] A. Borgna, R. F. Garetto, A. Monzon, C. R. Apesteguia, *Journal of Catalysis* **1994**, *146*, 69.

[67] J. Goetz, M. A. Vople, A. M. Sica, C. E. Gigola, E. Touroude, *Journal of Catalysis* **1997**, *167*, 314.

[68] H. D. Lanh, N. Khoai, H. S. Thoang, J. Volter, *Journal of Catalysis* **1991**, *129*, 58.

[69] P. D. Boyle, B. J. Johnson, B. D. Alexander, J. A. Casalnuovo, P. R. Gannon, S. M. Johnson, E. A. Larka, a. M. Mueting, L. H. Pignolet, *Inorg. Chem.* **1987**, *26*, 1346.

[70] L. N. Ito, A. M. P. Felicissimo, L. H. Pignolet, *Inorg. Chem.* **1991**, *30*, 387.

[71] L. N. Ito, J. D. Sweet, A. M. Mueting, L. H. Pignolet, M. F. J. Schoondergang, J. J. Steggerda, *Inorg. Chem.* **1989**, *28*, 3696.

[72] R. P. F. Kanters, J. J. Bour, P. P. J. Schlebos, W. P. Bosman, H. Behm, J. J. Steggerda, L. N. Ito, L. H. Pignolet, *Inorg. Chem.* **1989**, *28*, 2591.

[73] J. J. Bour, R. P. F. Kanters, P. P. Schlebos, J. J. Steggerda, *Recl. Trav. Chim. Pays-Bas* **1988**, *107*, 211.

[74] R. P. F. Kanters, P. P. J. Schlebos, J. J. Bour, W. P. Bosman, H. J. Behm, J. J. Steggerda, *Inorg. Chem.* **1988**, *27*, 4034. J. J. Bour, R. P. F. Kanters, P. P. J. Schlebos, W. P. Bosman, H. Behm, P. T. Beurskens, J. J. Steggerda, *Recl. Trav. Chim. Pays-Bas* **1987**, *106*, 157.

[75] J. J. Bour, P. P. J. Schlebos, R. P. F. Kanters, W. P. Bosman, J. M. M. Smits, P. T. Beurskens, J. J. Steggerda, *Inorg. Chim. Acta* **1990**, *171*, 177.

[76] M. F. J. Schoondergang, J. J. Bour, G. P. F. Van Strijdonck, P. P. J. Schlebos, W. P. Bosman, J. M. M. Smits, P. T. Beurskens, J. J. Steggerda, *Inorg. Chem.* **1991**, *30*, 2048.

[77] L. N. Ito, A. M. P. Felicissimo, L. H. Pignolet, *Inorg. Chem.* **1991**, *30*, 989.

[78] L. N. Ito, B. J. Johnson, A. M. Mueting, L. H. Pignolet, *Inorg. Chem.* **1989**, *28*, 2026.

[79] A. M. Mueting, W Bos, B. D. Alexander, P. D. Boyle, J. A. Casalnuovo, S. Balaban, L. N. Ito, S. M.Johnson, L. H. Pignolet, *New J. Chem.* **1988**, *12*, 505.

[80] J. H. Sinfelt, *Bimetallic Catalysis: Discoveries, Concepts and Applications*; J. Wiley & Sons: New York **1983**:pp 1-164 and references cited therein.

[81] B. C. Gates, L. Guczi, H. Knozinger, *Metal Clusters in Catalysis*; Elsevier: Amsterdam, **1988**.

[82] P. Braunstein, J. Rose. *In Stereochemistry of Organometallic and Inorganic Compounds*; I. Bernal, Ed; Elsevier: Amsterdam, **1988**; Vol. 3.

[83] M. A. Aubart, L. H. Pignolet, *J. Am. Chem. Soc.*, submitted for publication.

[84] Y. M. Shulga, A. V. Bulatov, R. A. T. Gould, W. V. Konze, and L. H. Pignolet, *Inorg. Chem.* **1992**, *31*, 4704-4706.

[85] M. J. Adrowski, W. R. Mason, *Inorg. Chem.* **1997**, *36*, 1443.

M. J. Adrowski, *Dissertation*, Northern Illinois University, **1996**.

[86] H. R. C. Jaw, W. R. Mason, *Inorg Chem.* **1991**, *30*, 275.

[87] W. R. Mason, *Inorg. Chem.* **2000**, *39*, 370-374

[88] F. A. Vollenbroek, J. J. Bour, J. M. Trooster, and J. W. A. Van der Belden, *J. Chem. Soc., Chem. Commun.*, **1978**, 907.

[89] F. A. Vollenbroek, W. P. Bosman, J. J. Bour, J. H. Noordik, and P. T. Beurskens, *J. Chem. Soc., Chem. Commun.*, **1979**, 387.

[90] F. A. Vollenbroek, J. P. Van Den Berg, J. W. A. Van Der Velden, and J. J. Bour, *Inorg. Chem.* **1980**, *19*, 2685-2688.

[91] F. Cariati and L. Naldini, J. Chem. Soc., *Dalton Trans.*, **1972**, 2286.

[92] P. M. T. M. Van Attekum, J. W. A. Van Der Velden and J. M. Trooster, *Inorg. Chem.* **1980**, *19*, 701-704.

[93] C. Battistoni, G. Mattogno, R. Zanoni, L. Naldini, *J. Electron Spectrosc. Relat. Phenom.* **1982**, *28*, 23.

[94] C. Battistoni, G. Mattogno, d. M. P. Mongos, *J. Electron Spectrosc. Relat. Phenom.* **1984**, *33*, 107.

[95] P. M. T. M. van Attekum, J. W. A. van der Velden, J. M. Trooster, *Inorg. Chem.* **1980**, *19*, 701.

[96] L. H. Pignolet, M. A. Aubart, K. L. Craighead, R. A. T. Gould, D. A. Krogsted, J. S. Wiley, *Coord. Chem. Rev.* **1995**, *143*, 219.

[97] D. Kummer, L. Diehl, *Angew. Chem., Int. Ed. Engl*. **1970**, *9*, 895.

[98] J. D. Corbett, D. G. Adolphson, D. J. Merryman, P. A. Edwards, F. J. Armatis, *J. Am. Chem. Soc.* **1975**, *97*, 6267.

[99] P. Edwards, J. D. Corbett, *Inorg. Chem.* **1977**, *16*, 903.

[100] W. L. Wilson, *Ph. D. Thesis(Wisconsin)*.

[101] R. W. Rudolph, W. L. Wilson, F. Parker, R. C. Taylor, D. C. Young, *J. Am Chem. Soc.* **1978**, *100*, 4629.

[102] R. W. Rudolph, R. C. Taylor, D. C. Young, *In Fundamental Reaearch in Homogeneous Catalysis*; M. Tsutsui, Ed.; Plenum Press: New Youk, **1979**, 997-1005.

[103] B. S. Pons, D. J. Santure, R. C. Tayor, R. W. Rudolph, *Electrochem. Acta.* **1981**, *26*, 365.

[104] W. L. Wilson, R. W. Rudolph, L. L. Lohr, R. C. Taylor, P. Pyykko, *Inorg. Chem.* **1986**, *25*, 1535.

[105] R. W. Rudolph, W. L. Wilson, *J. Am. Chem. Soc.* **1981**, *103*, 2480.

[106] J. Campbell, D. A. Dixion, H. P. A. Mercier, G. J. Schrobilgen, *Inorg. Chem.* **1995**, *34*, 5798-5809.

[107] J. Campbell, H. P. A. Mercier, H. Franke, D. P. Santry, D. A. Dixon, G. J. Schrobilgen, *Inorganic Chemistry* **2002**, *41*, 86.